Principles and algorithms of real-time sensing of motor action and psychophysiological state

Deliverable D3.1

List of Partners:	Swiss Federal Institute of Tech. Zurich, CH Hocoma AG, Volketswil, CH University of Ljubljana, SLO Universitat Politècnica de Catalunya, SPA Neurological Clinic Bad Aibling, D
Document Identifier:	MIMICS-D3.1-pu.pdf
Version:	3.0
Date:	2008-07-31
Organisation:	UL
Deliverable:	3.1
Milestone:	3.1
Workpackage:	3
Task:	3.1 & 3.2
Dissemination:	public
Authors:	Domen Novak, Matjaz Mihelj, Marc Bolliger, Alexander König, Jason Kastanis, Marko Munih
Approved by:	Lars Lünenburger, Mel Slater

Abstract: This report describes the real-time measurement of user's motor actions and measurement of psychophysiological state for both rehabilitation robotic system, the Lokomat and the HapticMaster.

Project Number: 215 756

Table of Contents

1 Summary

This is the D3.1 deliverable of the MIMICS project, funded by the European Community's Seventh Framework Programme under Grant Agreement n° 215756. In this report, we have documented a number of issues from work package 3 Multi-sensorial data processing and decision making required for the forthcoming collaborative research among the partners in the MIMICS project.
The output of task 3.1 *Principles and algorithms of real-time sensing of motor action and psychophysiological state* and task T3.2 *Real-time sensing of psychophysiological state* are the methods for real-time measurements of user's motor action in a systematic modular way and the measuring of physiological processes to obtain the subject's psychological state.

2 Real-time sensing of user motor actions

2.1 Introduction to the goals of measurements of user's motor actions

The results of this task are methods for real-time measurement of user's motor actions in a systematic modular way. Sensors acquire static and dynamic information such as forces/torques, positions and position derivatives, electromyographic (EMG) activity, as well as audio streams in order to record speech. Multi-sensorial integration algorithms were developed here in order to recognize the subject's voluntary motor activity and intention (intended movement direction) in real-time. Motor intentions are derived by an implicit approach by analysing force data. In an explicit approach intention can also be detected from voice commands (i.e. the user says what he wants). Particular aspects of this task include

- Signal acquisition, filtering and sensory integration: Measured data will be band-pass filtered and signals from different sensors will be integrated based on a dynamic model of human segmental biomechanics and Kalman estimator.
- Assessment of user's voluntary and involuntary muscle activity, and motor intentions: User's voluntary and involuntary activity will be estimated through comparison of the user's motor activity with the predictions from dynamic models and measurements of healthy subjects performing the same task. Movement intentions will be estimated from the force and EMG data.

2.2 Measurement set-up (HapticMaster)

Measurement set-up for HapticMaster includes various sensors and sensory systems for measuring robot joint positions and velocities, forces, accelerations and angular rates. The basic set-up is shown in Figure 1.

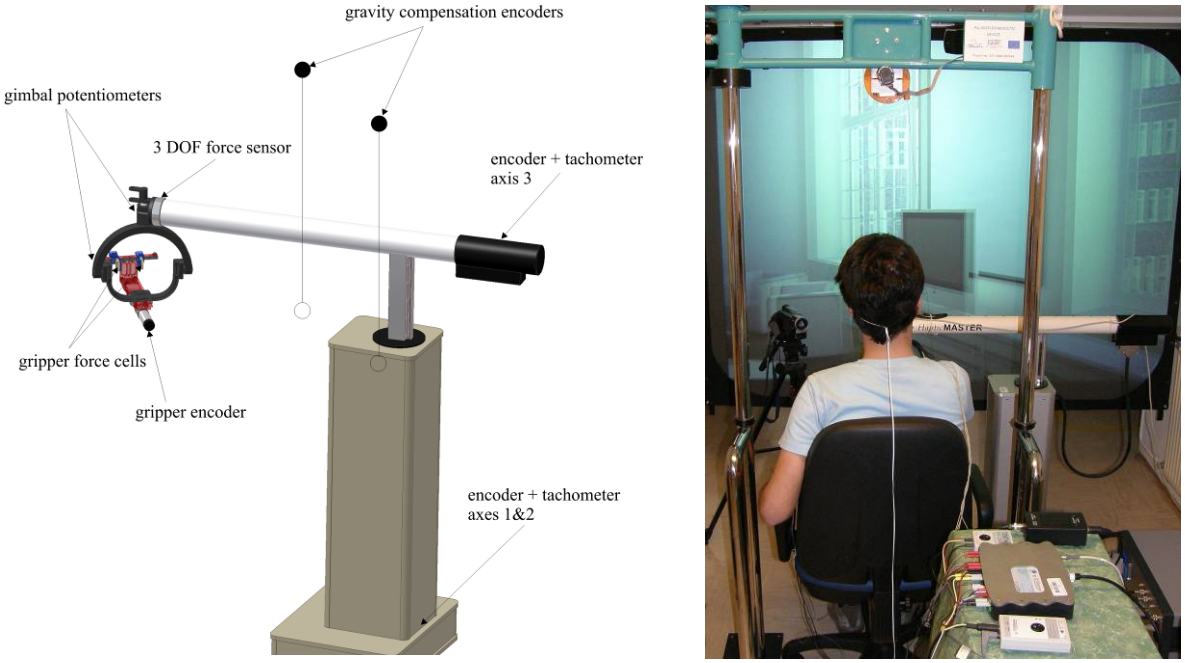

Figure 1 Measurement of user's motor actions; sensors built in and around the HapticMaster robot (left figure); MIMICS upper extremity system - back view of the subject training with HapticMaster robot; system components visible in the picture: robot, 3D projection screen (behind), camcorder (left behind), system for measurement of psychophysiological signals (in front), gravity compensation device attached above the subject and connected to the subject's arm (elbow cuff) via a thin Kevlar wire (not visible in the image).

2.2.1 Position sensors

Robot joint encoders, tachometers and potentiometers (gimbal)

These sensors are built in the original HapticMaster (Moog FCS, Inc.) robot. Each robot axis is equipped with an encoder for measuring joint angles and a tachometer for measuring joint velocities. Encoder signals are available to the user, while tachometer signals are only used in the hardware based velocity control loop and cannot be accessed from the control application. Two gimbal passive axes are equipped with potentiometers, which signals are available to the user.

Gravity compensation encoders

Gravity compensation system is an active system equipped with two rotary motors. Each motor is equipped with an encoder with a resolution of 512 counts per revolution, which equals 137 counts per millimeter. Encoder outputs are used within the controller for implementing the arm gravity compensation.

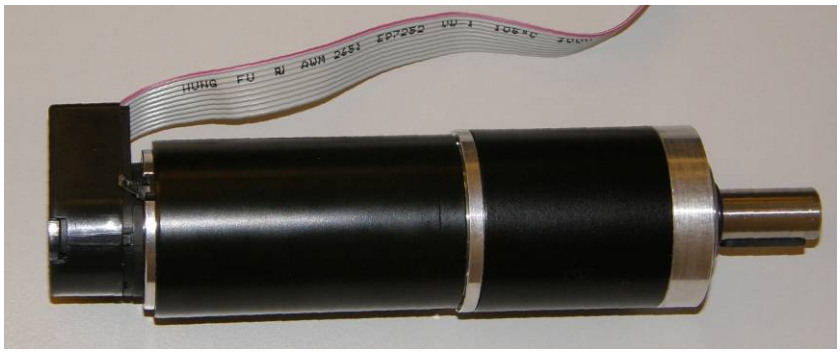

Figure 2 Motor with encoder attached at the left side. A similar system is used also for the grasping device, only with a smaller motor

Grasping device encoder

Grasping device is an active system with one degree of freedom used for training of opening and closing of fingers. It is actuated using a rotary motor equipped with an encoder with a resolution of 512 counts per revolution, which equals 154 counts per millimeter. Encoder signals enable measurement of opening and closing of fingers. This is then used for the design of various control strategies for training of grasping.

2.2.2 Force sensors

Robot end-effector force sensors

A 3 axes force sensor is originally built in the HapticMaster robot. The sensor enables measurement of the three-dimensional components of forces acting on the robot end-effector. These measured forces are available to the user to be used in the robot control system.

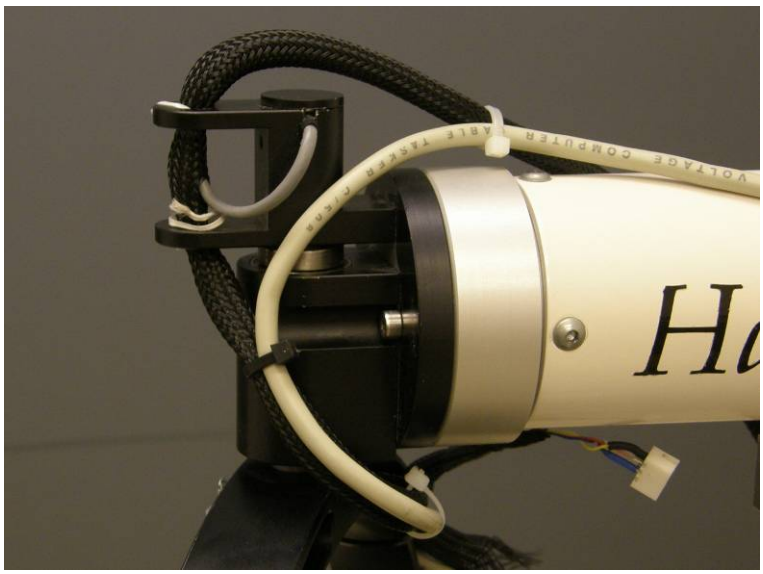

Figure 3 Robot end-effector force sensor. One of gimbal potentiometers is partially also visible.

Grasping device force cells

The device for training of grasping is equipped with two one axis (compression/extension) load cells. The load cells are positioned between the fingers and the respective finger attachments on the device itself. Each force cell is capable of measuring forces up to 100 N, which is enough for training applications envisioned

for rehabilitation. The signals from the load cells are interfaced to the robot controller and are available to the user.

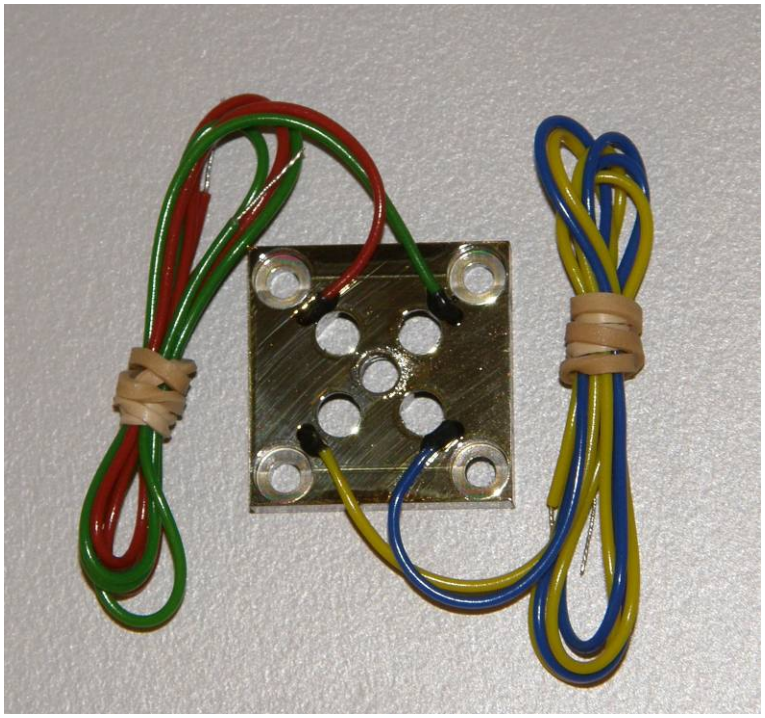

Figure 4 One axis compression/extension load cell

2.2.3 Inertial sensors

Accelerometers and gyroscopes on the upper arm

Human arm is a redundant system concerning the spatial relation of hand and shoulder location) with seven active degrees of freedom (if we use the simplest model: three in the shoulder joint, one in the elbow joint and three in the wrist joint). It is therefore impossible to compute inverse kinematics (joint angles) of the arm based only on the hand position. In order to find the unique solution additional information is required. For this purpose, an inertia measurement system attached to the upper arm is used. This system consisting of three accelerometers and three gyroscopes was developed at UL. Output of the system allows for the estimation of the upper arm orientation, and together with the hand position the arm inverse kinematics.

2.2.4 Speech sensors

A common off-the-shelf headset with an attached microphone is placed on the subject's head and used to record speech for further analysis.

2.2.5 Camcorder

Camcorder for visual inspection of measurements

A consumer-product camcorder (resolution: 640x480 pixels) is placed in front of the subject recording the movements, gestures and face expressions. The resulting data

will be visually inspected and manually correlated with the measured data. The information from the camcorder will allow verification of algorithms for automatic behaviour and emotion detection. Data from the camcorder will not be used in any automatic control strategy.

The complete set of sensors for the HapticMaster setup is shown in Figure 5.

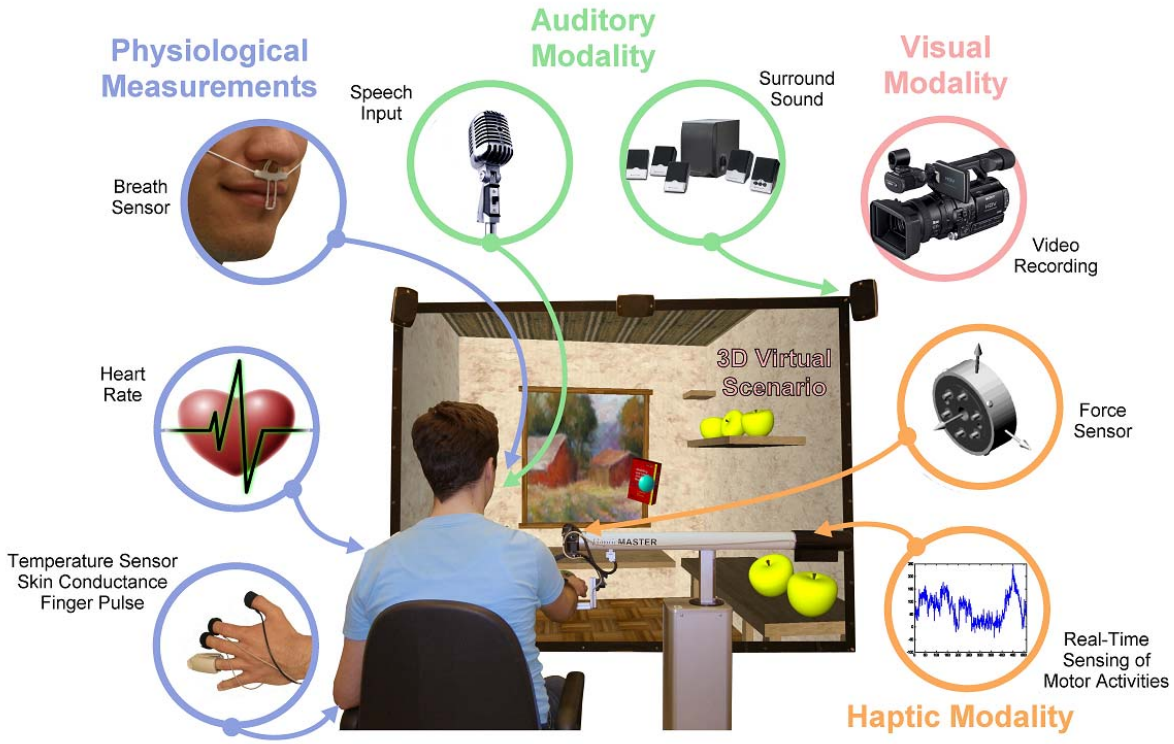

Figure 5 The complete HapticMaster measurement set-up

2.3 Measurement set-up (Lokomat)

The Lokomat® Pro systems (Hocoma AG, Volketswil, Switzerland) used in this project is equipped with several sensors that are used to assess patients' activity. Figure 6 shows the basic setup of the Lokomat leg orthosis.

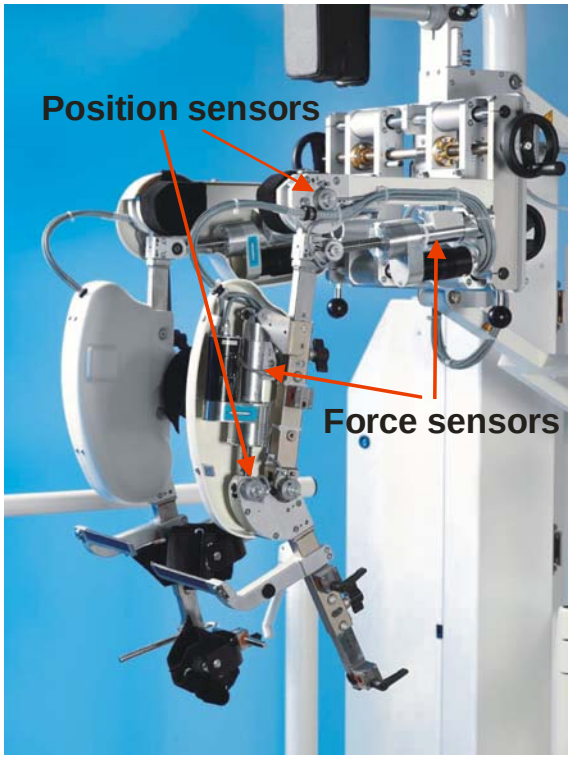

Figure 6 The driven gait orthosis Lokomat with sensors to measure patients' motor activity (modified from photo courtesy of Hocoma AG, Volketswil, Switzerland)

2.3.1 Position sensors

A redundant pair of position sensors is mounted for each joint (hip and knee, left and right). All sensors for all joints are of the same type. Exact manufacturer details can be seen in Deliverable 1.2.

2.3.2 Force sensors

Four force sensors, one in each joint are implemented. The exact manufacturer details can be seen in Deliverable 1.2.

Additional force-sensors (Kistler) are mounted in the treadmill (gaitway II by h/p/cosmos, Nussdorf-Traunstein, Germany) measuring ground reaction forces in the anterior and posterior half of the walking surface.

2.3.3 Speech sensors

One standard consumer-product microphone is used for speech recording.

2.3.4 Camcorder

Standard DV camcorder for visual off-line inspection of measurements.

The complete set of sensors for the Lokomat setup is shown in Figure 7.

Figure 7: The complete Lokomat measurement set-up

2.4 Signal acquisition

2.4.1 Electronics hardware architecture

HapticMaster robot

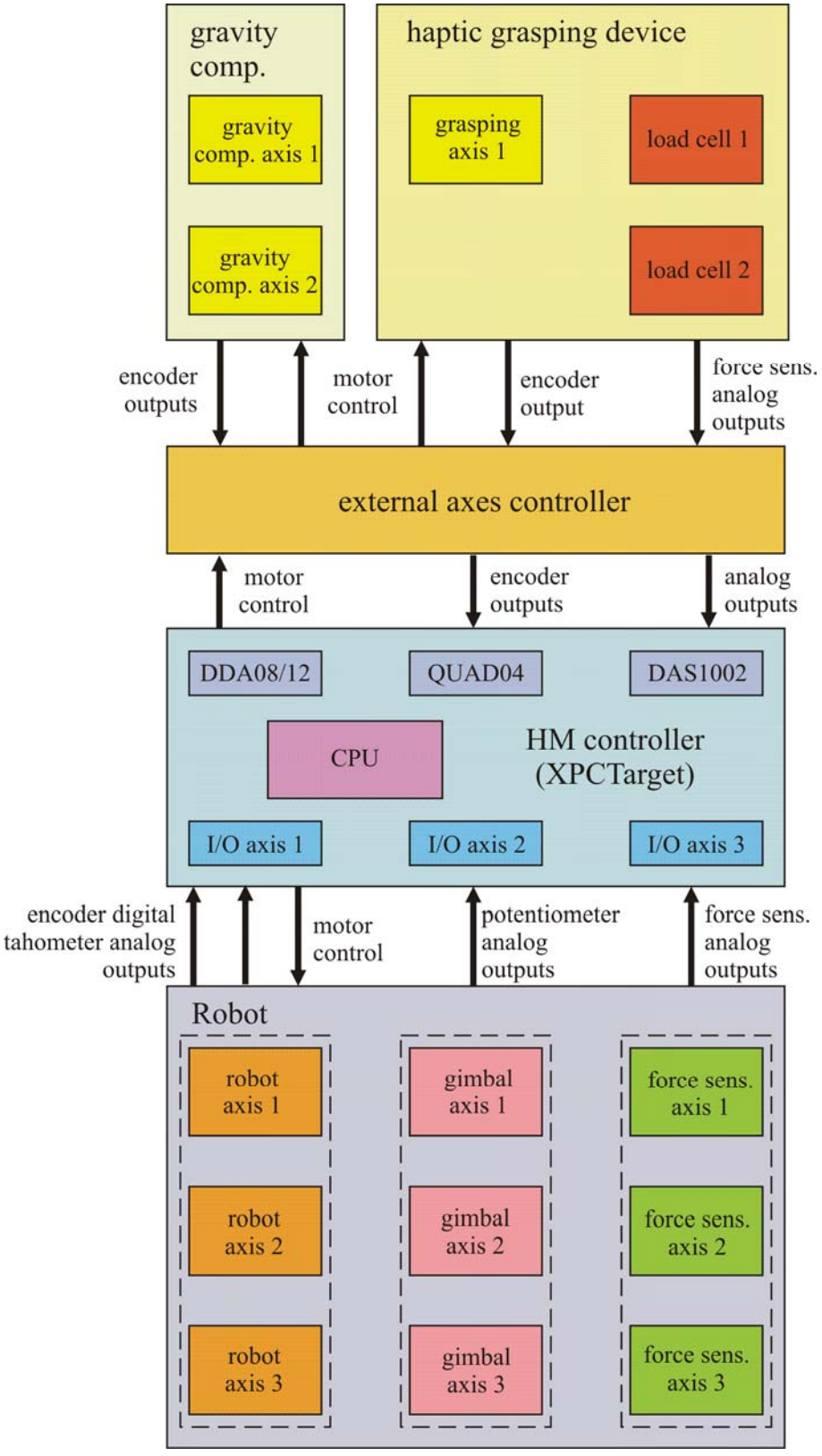

Figure 8 Block diagram of HapticMaster electronics hardware architecture

Signals from sensors described in section 1.2 are interfaced to the robot controller through various input/output interface cards inserted in the HapticMaster control PC. Signals from robot position and force sensors are directly connected to the robot's three-axes modules, which control all three axis movements. In order to acquire the auxiliary sensors signals (encoders for gravity compensation and grasping device, grasping device load cells, inertial measurement system, EMG signals) MeasurementComputing interface boards in the HapticMaster control PC are used. Two additional acquisition boards are used for measuring analog signals (PCI-DAS1002) and encoder signals (PCI-QUAD04) respectively.

Figure 9 PCI-DAS1002 - High-Speed PCI-bus compatible, 12-bit, 16-Channel Analog Input Board with Dual Analog Output Channels & 24 Digital I/O bits (photo: www.measurementcomputing.com)

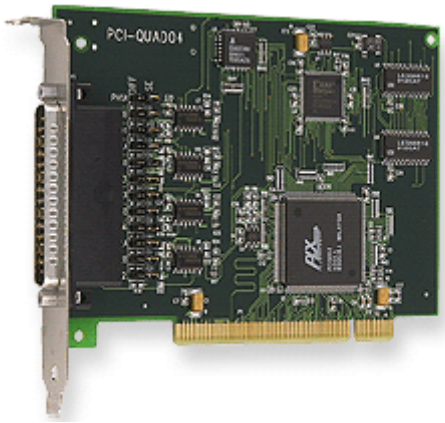

Figure 10 PCI-QUAD04 - 4 Channel quadrature encoder board (photo: www.measurement-computing.com)

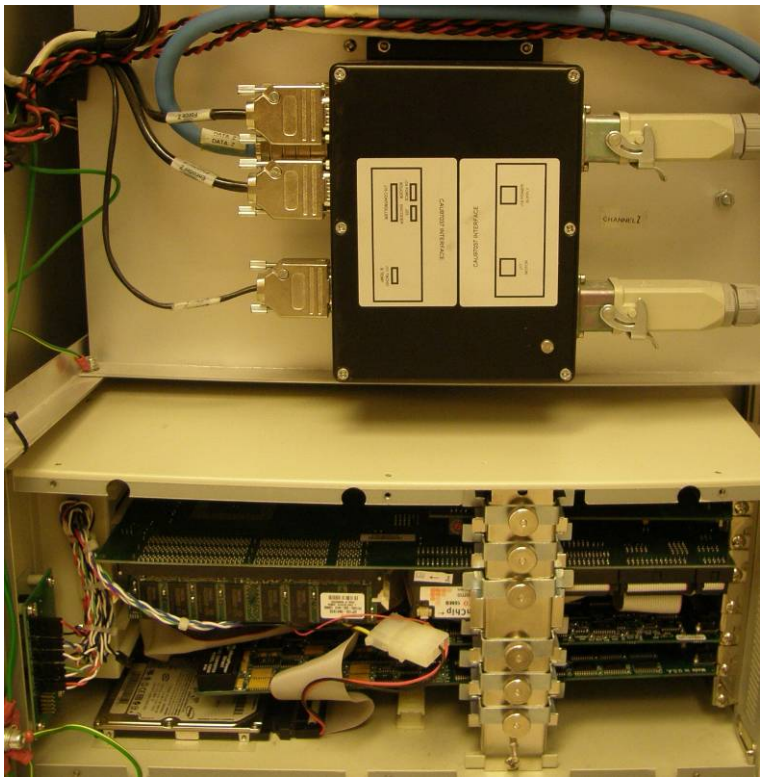

Figure 11 Partial view of the robot controller. The controller for one robot axis with all input/output interfaces is visible in the upper half of the picture. Below the controller motherboard the MeasurementComputing interface cards are visible.

2.4.2 xPC Target interface

In order for the sensory signals to be used in the robot control software, the sensor outputs need to be acquired in Matlab xPC Target environment, which is used for the implementation of the controller. The original HapticMaster controller is implemented in VXWorks real-time operating system. Therefore, the drivers for acquisition of robot position and force data were rewritten for Matlab xPC Target. The new driver is implemented as a Simulink block, which is designed to be executed in real-time applications. Its output provides position information for the two translational and one rotational joint, three gimbal rotation axes as well as the three-dimensional force components at the end-effector of the robot. This data set describes the state of the manipulator completely and is suitable for subsequent application demands.

The PCI-DAS1002 and PCI-QUAD04 interface boards are generically supported in Matlab xPC Target environment (one of the main criteria for choosing these interface boards).

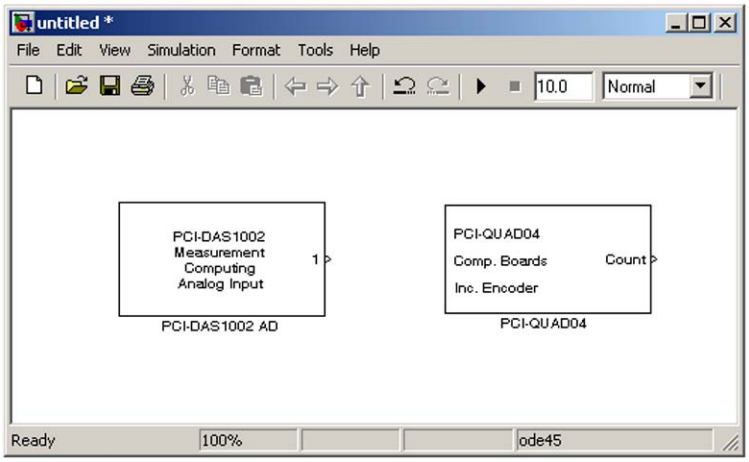

Figure 12 Matlab xPC Target blocks for interfacing Measurement computing boards

Sampling of all signals is done at 2.5 kHz sampling frequency, which is also the sampling frequency of the robot controller.

2.4.3 Speech recording

A large amount of speech recording software exists for all platforms, including some programs built into Windows. Dragon NaturallySpeaking 9.0 (described in section 1.5.4) was selected for direct analysis and interpretation.

2.5 Signal analysis and interpretation

2.5.1 Basic signal filtering (noise removal)

Basic signal filtering is required to remove high frequency noise that could affect the controller performance, while at the same time preserving information arising from human movement. Since the sampling frequency of all signals is at least 1 kHz, the cut-off frequency of filtered signals was set to 30Hz, which is beyond the maximum frequency of human movement.

2.5.2 Removal of artefacts

The Lokomat itself is shielded well enough to not influence the targeted psychophysiological signals. Artefacts in the ECG and electrodermal activity signals that arise from electrostatic charging due to friction with the treadmill can be removed by attaching a ground strap around the wrist and connecting the strap to the common signal ground.

In order to verify that the Lokomat does not produce artefacts, we recorded electrodermal activity (galvanic skin response, GSR) in four different conditions while a healthy subject (i) walked on the treadmill with 2.1 km/h being grounded and (ii) without grounding and (iii) stepping in place (treadmill switched off) with and (iv) without grounding. Figure 13 shows examples of the recordings.

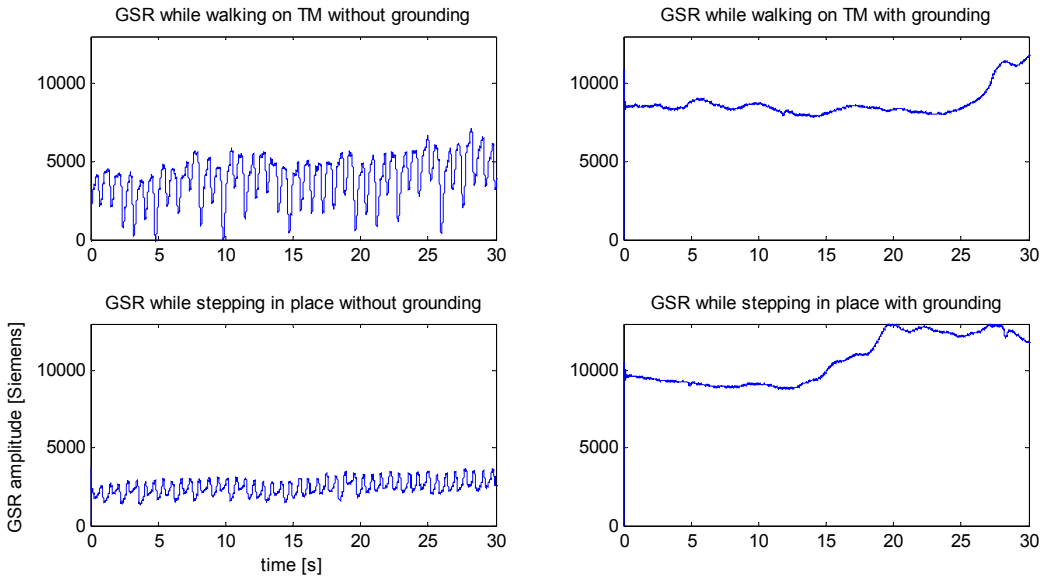

Figure 13 Signal artefacts on the Lokomat

Peaks in the corresponding power-spectra (cf. Figure 14) correspond to the used walking and stepping cadence and thus verify the movements as the source of the artefact.

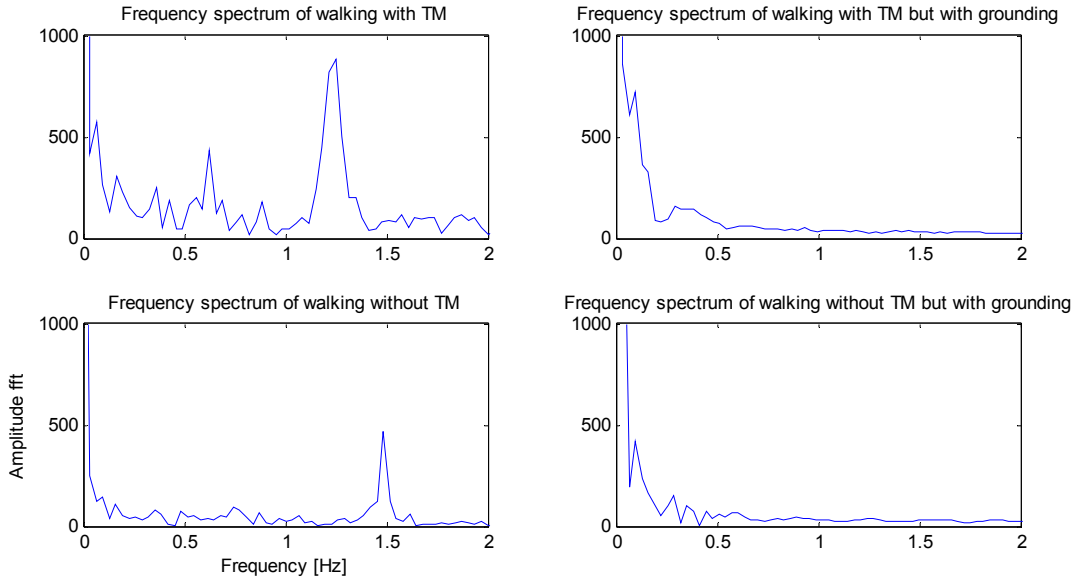

Figure 14 Frequency spectrums of electrodermal activity while walking

2.5.3 Voluntary and involuntary muscle activity for Lokomat

Voluntary muslce activity can be specified by the biofeedback values, weighted force measurements from the force sensors. The biofeedback values can be used to assess paitients activity. To improve the accuracy of the biofeedback a new method was developed. The new method bases on empirical data that were obtained from healthy subjects when simulating distinctive degrees of walking performance during robot-assisted gait training. This empirical data-based biofeedback (EDBF) method was evaluated with 18 subjects without gait disorders. A higher correlation between the subjects' walking performance and biofeedback values was found for the EDBF method compared to the conventional theory-based biofeedback approach (for details, see [Banz, 2008]).

Calculation of biofeedback values [Banz, 2008]

Biofeedback is calculated for the hip and knee during stance and swing phase according to the following equation:

$$FB_{j,p} = \sum_{a} \left(fb_{a_{j,p}} \cdot s(a) \right) + z_{j,p} \tag{1}$$

where FB is the biofeedback value, j is the joint with j =1 for hip and j = 2 for knee, p is the gait phase with p = 1 for stance and p = 2 for swing, a is a subsection of the gait cycle, fb is the biofeedback value for a subsection of the gait cycle, s is a factor to assign a positive or negative sign to the biofeedback value and z is a constant to compensate the offset for the passive components of the DGO.

The biofeedback values of the different subsections of the gait cycle fb(a) are calculated according to the following equation:

$$fb_{a_{j,p}} = \frac{\sum_{k} \left(c_{j,p}[k] \cdot \left(y_j[k] - r_j^{active}[k] \right) \right)}{\sum_{k} c_{j,p}[k]} \tag{2}$$

where c is a weighting function and k is the time point during the gait cycle with k = {1, 500} for the stance phase and k = {550, 1000} for the swing phase, y is the measured man-machine interaction force and r^{active} is the active reference force curve. The difference between the measured interaction force curve y[k] and the reference interaction force curve r[k] is calculated for each time point during the step cycle k in order to determine the deviation of the measured interaction force curve of a subjects from the "ideal" walking performance. The difference y[k] - r^{active}[k] is multiplied by a corresponding weighting function c[k].

Stance and swing phase are divided into subsections a in order to judge the biofeedback values, i.e. to assign positive biofeedback values for desired and negative biofeedback values for unsatisfactory walking performance. Four cases are differentiated, where the sections a are determined by the constellation of the algebraic signs of the functions c[.] and r^{active}[.]:

$$\left.\begin{array}{l} r^{active}[.] \le 0 \\ c[.] \le 0 \end{array}\right\} \; y[.] \le r^{active}[.] \rightarrow positive \;\; fb_a \tag{3.1}$$

$$\left.\begin{array}{l} r^{active}[.] \le 0 \\ c[.] > 0 \end{array}\right\} \; y[.] \ge r^{active}[.] \rightarrow positive \;\; fb_a \tag{3.2}$$

$$\left.\begin{array}{l} r^{active}[.] > 0 \\ c[.] \le 0 \end{array}\right\} \; y[.] \le r^{active}[.] \rightarrow positive \;\; fb_a \tag{3.3}$$

$$\left.\begin{array}{l} r^{active}[.] > 0 \\ c[.] > 0 \end{array}\right\} \; y[.] \ge r^{active}[.] \rightarrow positive \;\; fb_a \tag{3.4}$$

The factor s(a) in equation (1) is s(a) = 1 in case of the constellations described in (3.2) and (3.4) and s(a) = -1 in case of the constellations described in (3.1) and (3.3). This procedure assures that desired walking performance results in fb_a s(a) ≥ 0 which corresponds to a positive biofeedback value.

Weighting functions

$$c_{j,p}[k] = \frac{r_{j,p}^{active}[k] - r_{j,p}^{passive}[k]}{\max\left\{r_{j,p}^{active}[k'] - r_{j,p}^{passive}[k']\right\}} \tag{4}$$

The weighting functions were constructed by calculating the difference between the “active” interaction force reference curve ractive[k] and the “passive” interaction force reference curve $r^{passive}$[k] at any time during the gait cycle. The normalization with the divisor was conducted separately for the stance phase with k’ = {1,500} and swing phase with k’ = {550,1000} of the hip (j = 1) and knee joint (j = 2). With this procedure, the observed force difference determined the amplitude of the weighting function for each time point within the gait cycle, i.e. the sections with the highest observed interaction force differences were weighted the highest

The biofeedback values can be directly provided to the patient via graphical feedback. A second way is to couple the biofeedback to the treadmill speed. If the patient exerts force onto the Lokomat orthosis in a therapeutically desired way, the treadmill will accelerate. If the forces exerted by the patient are not therapeutically desired, the voluntary muscle forces will decelerate the treadmill.

Estimation of arm inverse kinematics based on inertial measurements and robot measurements

A technique for computation of the inverse kinematic model of the human arm was developed. The approach is based on measurements of the hand position and orientation as well as translational acceleration and angular rate of the upper arm segment. A quaternion description of orientation is used to avoid singularities in representations with Euler angles. A Kalman filter was designed to integrate sensory data from three different types of sensors. The algorithm enables estimation of human arm posture, which can be used in trajectory planning for rehabilitation robots, evaluation of motion of patients with movement disorders, and generation of virtual reality environments.

The human arm can be modelled as a seven-degree-of-freedom mechanism (Figure 15) consisting of the shoulder ball–and–socket joint, the elbow revolute joint, and the wrist ball–and–socket joint.

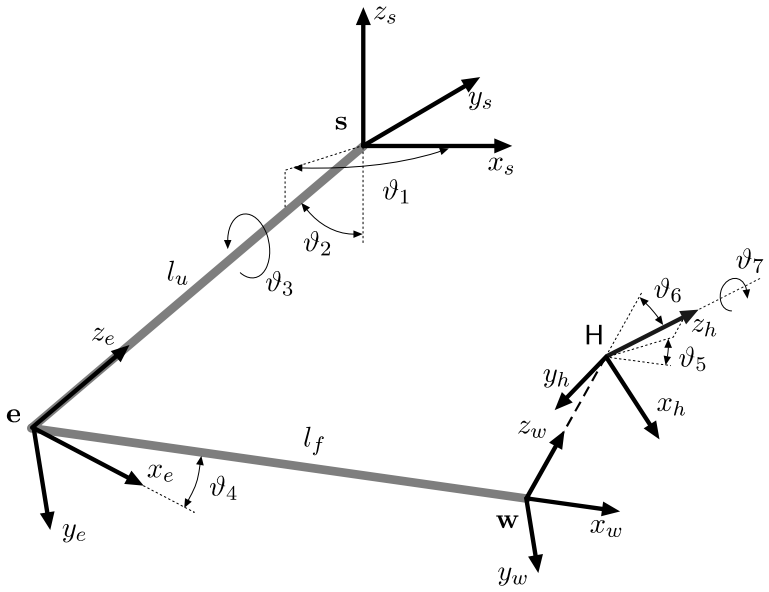

Figure 15 Simplified kinematic model of the human arm with 7 degrees of freedom.

The kinematic chain contains seven joint variables, therefore it has one redundant degree of freedom when given only the position and the orientation of the hand. A simple physical interpretation of the redundant degree of freedom is that the elbow is still free to swivel about a circular arc whose normal vector is parallel to the straight line connecting the shoulder and the wrist. Based on relations in Figure 15, the following arm transformation matrices can be defined

$$\mathsf{T}_s = rot(z_s, \vartheta_1) rot(x_s, \vartheta_2) rot(z_s, \vartheta_3) tr(z_s, -l_u)$$

$$\mathsf{T}_e = rot(z_e, \frac{\pi}{2}) rot(x_e, \vartheta_4) rot(z_e, -\frac{\pi}{2}) tr(x_e, l_f)$$

$$\mathsf{T}_w = rot(z_w, \vartheta_5) rot(x_w, \vartheta_6) rot(z_w, \vartheta_7),$$

Figure 16 shows measurements available for the estimation process. The position and orientation of the hand is computed from the robot direct kinematic model because the hand is tightly coupled to the robot end-effector. In addition matrix acceleration and angular rate of the upper arm are measured using a triad of accelerometers and a triad of gyroscopes. The accelerometer output signal strongly depends on its position of the sensors on the upper arm.

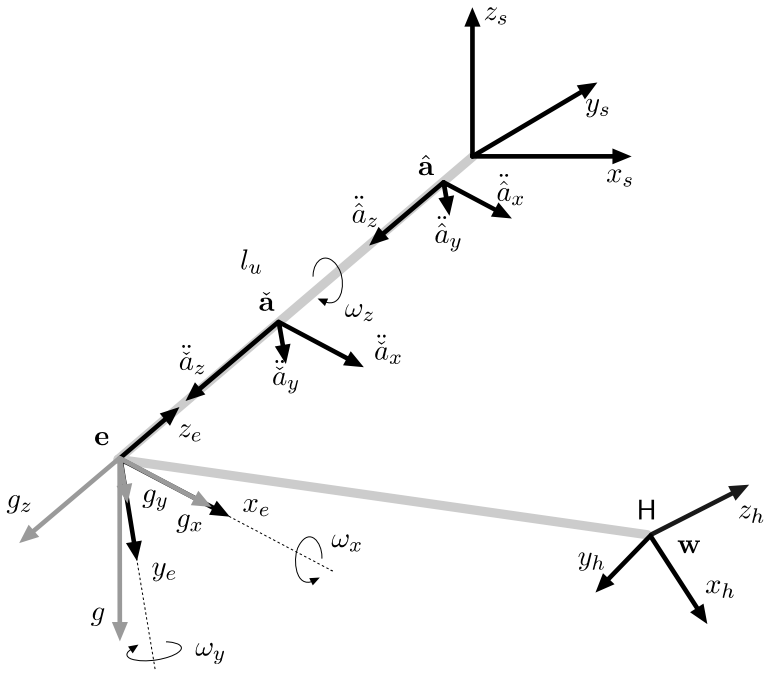

Figure 16 Available measurements: hand pose, upper arm angular rate, upper arm accelerations

If the position of the shoulder joint is fixed and we assume the attachment point of the accelerometer close to the straight line connecting shoulder and elbow joints, is the measured acceleration at a point

$$\ddot{\hat{\mathbf{a}}}=\begin{bmatrix} gs_2s_3+L_{\hat{a}}\left((\frac{1}{2}\dot{\vartheta}_1^2s_{22}-\ddot{\vartheta}_2)s_3+(2\dot{\vartheta}_1\dot{\vartheta}_2c_2+\ddot{\vartheta}_1s_2)c_3\right) \\ gs_2c_3+L_{\hat{a}}\left((\frac{1}{2}\dot{\vartheta}_1^2s_{22}-\ddot{\vartheta}_2)c_3-(2\dot{\vartheta}_1\dot{\vartheta}_2c_2+\ddot{\vartheta}_1s_2)s_3\right) \\ gc_2-L_{\hat{a}}\left(\dot{\vartheta}_1^2s_2^2+\dot{\vartheta}_2^2\right) \end{bmatrix}$$

A quaternion may be used to rotate a 3-dimensional vector using quaternion multiplications

$$\mathbf{u}_{rot} = Q^* \otimes \mathbf{u} \otimes Q$$

Equation can be rewritten in terms of rotation matrix as

$$\mathbf{u}_{rot} = \mathsf{M}(Q)\mathbf{u}$$

$$\mathsf{M}(Q) = \frac{1}{\|Q\|}\begin{bmatrix} 1-2(q_2^2+q_3^2) & 2(q_1q_2+q_3q_0) & 2(q_1q_3-q_2q_0) \\ 2(q_1q_2-q_3q_0) & 1-2(q_1^2+q_3^2) & 2(q_2q_3+q_0q_1) \\ 2(q_1q_3+q_2q_0) & 2(q_2q_3-q_1q_0) & 1-2(q_1^2+q_2^2) \end{bmatrix}$$

Next we define an operator that relates the Euler angles notation to a unit quaternion description of orientation as

$$\begin{aligned} \mathcal{T}(\mathbf{\Lambda}) = Q &= \begin{bmatrix} q_0 & q_1 & q_2 & q_3 \end{bmatrix} \\ \mathbf{\Lambda} &= \begin{bmatrix} \lambda_1 & \lambda_2 & \lambda_3 \end{bmatrix}^T \\ q_0 &= \cos\tfrac{\lambda_2}{2}\cos\tfrac{\lambda_1+\lambda_3}{2} \\ q_1 &= \sin\tfrac{\lambda_2}{2}\cos\tfrac{\lambda_1-\lambda_3}{2} \\ q_2 &= \sin\tfrac{\lambda_2}{2}\sin\tfrac{\lambda_1-\lambda_3}{2} \\ q_3 &= \cos\tfrac{\lambda_2}{2}\sin\tfrac{\lambda_1+\lambda_3}{2} \end{aligned}$$

Next, we will write the position of the wrist using the quaternion notation. The analysis is based on relations in Figure 17. We start with the supposition that the elbow joint angle represents the only joint variable that affects the distance between the shoulder and the wrist. For the given elbow flexion/extension we assume the initial position of the wrist exactly below the shoulder joint, as in Figure 17a. Next we perform a rotation in terms of Euler angles

$$\mathbf{\Phi} = \begin{bmatrix} \varphi_1 & \varphi_2 & \varphi_3 \end{bmatrix}^T$$

to place the wrist in a position where all shoulder angles equal zero (see Figure 17b). The final wrist position in Figure 17c can be obtained if actual shoulder angles

$$\mathbf{\Theta}_s = \begin{bmatrix} \vartheta_1 & \vartheta_2 & \vartheta_3 \end{bmatrix}^T$$

are considered. The last two rotations can be written in terms of quaternions as

$$\begin{aligned} Q_t &= \mathcal{T}(\mathbf{\Phi}) \\ Q_s &= \mathcal{T}(\mathbf{\Theta}_s) \end{aligned}$$

The actual wrist position can be obtained as a sequence of two rotations starting from the position exactly below the shoulder joint as

$$\mathbf{w} = Q_s \otimes Q_t \otimes \mathbf{w}_0 \otimes Q_t^* \otimes Q_{s.}^*$$

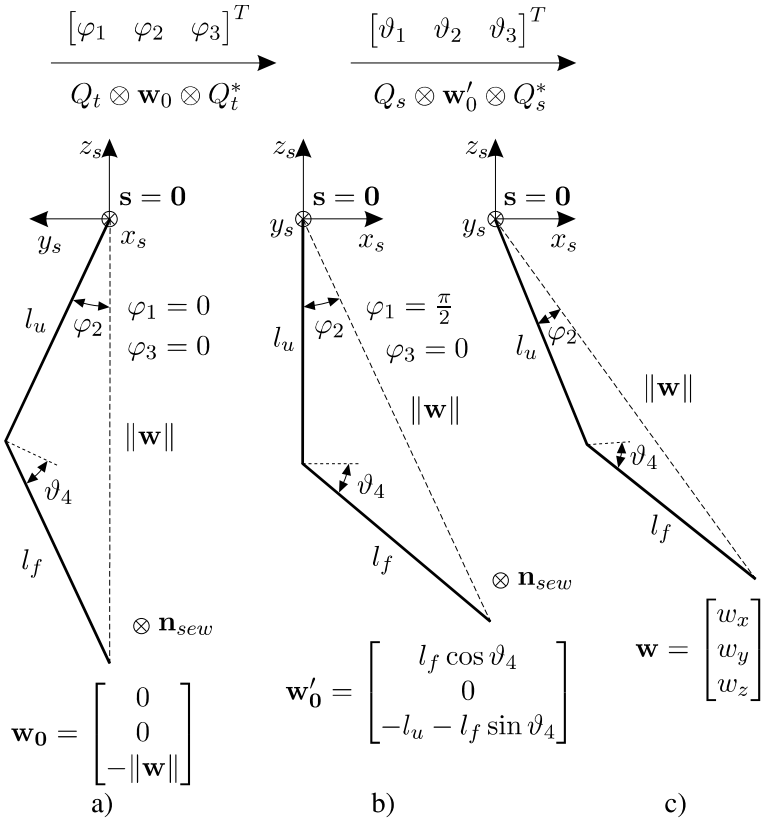

Figure 17 Graphical representation of the shoulder joint rotation sequence from an initial posture a), through an intermediate posture b), to the actual arm posture c).

We define a vector of available measurements including acceleration data and wrist position as

$$\mathbf{y} = \begin{bmatrix} \mathbf{g}^T & \mathbf{w}^T \end{bmatrix}^T$$

and the vector of measurement estimates as

$$\begin{aligned} \hat{\mathbf{y}} &= \begin{bmatrix} \hat{\mathbf{g}}^T & \hat{\mathbf{w}}^T \end{bmatrix}^T \\ \hat{\mathbf{g}} &= \hat{Q}_s^* \mathbf{g}_0 \hat{Q}_s \\ \hat{\mathbf{w}} &= \hat{Q}_s \otimes Q_t \otimes \mathbf{w}_0 \otimes Q_t^* \otimes \hat{Q}_s^* \\ \mathbf{g}_0 &= \begin{bmatrix} 0 & 0 & -g \end{bmatrix}^T \end{aligned}$$

The error between the actual measurement and its estimate is the input signal to the estimation of the new upper arm attitude quaternion. Therefore, we define the estimation error vector as

$$\boldsymbol{\Upsilon} = \mathbf{y} - \hat{\mathbf{y}}$$

We begin the estimation process with an initial estimate and use the estimation error vector to calculate the next estimate. The small rotation from the current estimated attitude to the next estimated attitude is defined as an error quaternion. If the rotation

angle is small, the so called error quaternion may be used for the purpose of rotation, and it is obtained by dividing the unit quaternion by its scalar part

$$Q_v = \frac{\cos\frac{\theta}{2} + \mathbf{r}\sin\frac{\theta}{2}}{\cos\frac{\theta}{2}} = 1 + \mathbf{r}\tan\frac{\theta}{2}$$
$$= \begin{bmatrix} 1 & v_1 & v_2 & v_3 \end{bmatrix} = \begin{bmatrix} 1 & \mathbf{v}^T \end{bmatrix}$$

The error quaternion is small but non-zero, due to errors in the various sensors. The relationship is expressed in terms of quaternion multiplication

$$\hat{Q}_{s^+} = \hat{Q}_s \otimes \begin{bmatrix} 1 & \mathbf{v}^T \end{bmatrix} = \hat{Q}_s \otimes Q_v$$

The goal of the estimation process is the minimization of the error vector. We define a Jacobian that relates the estimation error vector to the error quaternion as

$$\mathsf{J}(\mathbf{v}) = -\frac{\partial \hat{\mathbf{y}}(\mathbf{v})}{\partial \mathbf{v}} = -\begin{bmatrix} \frac{\partial \hat{\mathbf{y}}(\mathbf{v})}{\partial v_1} & \frac{\partial \hat{\mathbf{y}}(\mathbf{v})}{\partial v_2} & \frac{\partial \hat{\mathbf{y}}(\mathbf{v})}{\partial v_3} \end{bmatrix}$$
$$= -\begin{bmatrix} \mathbf{j}_1(\mathbf{v}) & \mathbf{j}_2(\mathbf{v}) & \mathbf{j}_3(\mathbf{v}) \end{bmatrix}.$$

$$\mathbf{j}_i(\mathbf{v})|_{\mathbf{v}=0} = \begin{bmatrix} \frac{\partial \mathsf{M}(Q_v)}{\partial v_i}|_{\mathbf{v}=0}\hat{\mathbf{g}} \\ \mathsf{M}(\hat{Q}_s)^T \frac{\partial \mathsf{M}(Q_v)^T}{\partial v_i}|_{\mathbf{v}=0}\mathsf{M}(\hat{Q}_s)\hat{\mathbf{w}} \end{bmatrix}$$

Using the above defined Jacobian matrix we can now write the following relations

$$\boldsymbol{\Upsilon} = -\mathsf{J}(\mathbf{v})\mathbf{v}$$
$$Q_v = \begin{bmatrix} 1 & -((\mathsf{J}(\mathbf{v})^T\mathsf{J}(\mathbf{v}))^{-1}\mathsf{J}(\mathbf{v})^T\boldsymbol{\Upsilon})^T \end{bmatrix}$$
$$\hat{Q}_{s^+} = \hat{Q}_s \otimes \begin{bmatrix} 1 & -((\mathsf{J}(\mathbf{v})^T\mathsf{J}(\mathbf{v}))^{-1}\mathsf{J}(\mathbf{v})^T\boldsymbol{\Upsilon})^T \end{bmatrix}$$

Finally, we have to formulate the Kalman filter for the estimation of arm kinematics. Let the following equation describe a single axis gyroscope model (we consider actual angular rate, a bias signal and the sensor noise)

$$\xi = \omega + b + n_w$$

The quaternion Q_s may be treated as a measurement available to the Kalman filter. Combined with the angular rate measurements

$$\boldsymbol{\Xi} = \begin{bmatrix} \xi_x & \xi_y & \xi_z \end{bmatrix}^T$$

the Kalman filter has a total of seven measurements. We define a system state vector as

$$\mathbf{x} = \begin{bmatrix} \mathbf{\Omega} \\ \mathbf{b} \\ Q_s \end{bmatrix}$$

$$\mathbf{\Omega} = \begin{bmatrix} \omega_x & \omega_y & \omega_z \end{bmatrix}^T$$

$$\mathbf{b} = \begin{bmatrix} b_x & b_y & b_z \end{bmatrix}^T$$

The derivatives of the state vector x are as follows

$$\dot{\mathbf{\Omega}} = \frac{1}{\tau}(\mathbf{\Omega} + \mathbf{n}_w)$$

$$\dot{\mathbf{b}} = \mathbf{0}^{3\times 1}$$

$$\dot{Q}_s = \frac{1}{2}\mathbf{\Omega} \otimes Q_s$$

A block scheme of the complete estimation process is shown in Figure 18.

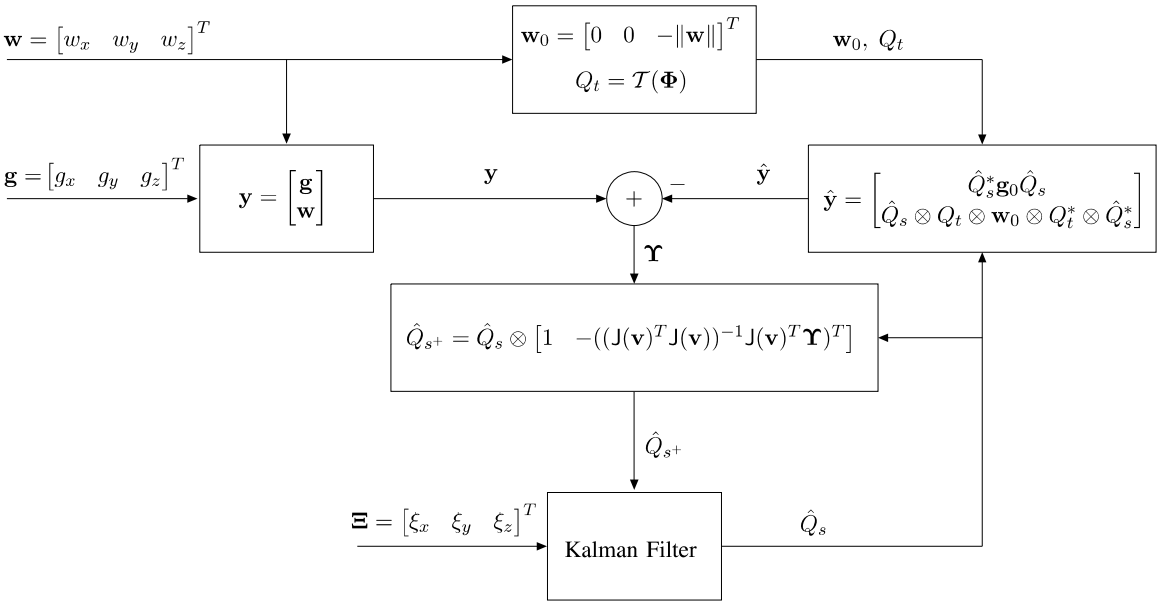

Figure 18 Estimation of the upper arm attitude quaternion Qs.

The results of the estimation process are shown in Figure 19.

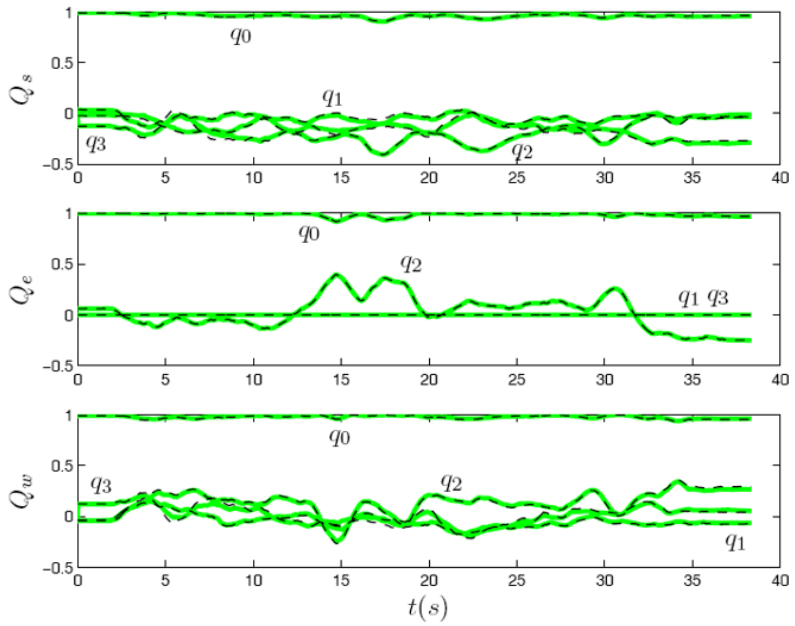

Figure 19 Results of the estimation process; reference (dashed line) and estimated values of shoulder, elbow and wrist quaternions.

Estimation of required gravity compensation for the human arm

The patient cooperative control strategy supports the movement of the hand toward the target posture. At the same time it allows the subject to choose his preferred movement trajectory. The drawback of the proposed controller is that if the patient is not fit enough to support the weight of the arm, which is often the case, the movement trajectory would be shaped by the influence of gravity. Movements would generally not be directed toward the target, but the arm would first tend to move downward due to its weight. To solve this issue an adaptive gravity compensation algorithm is proposed that controls the arm weight support based on the patient's performance. The weight of the robot is inherently compensated by the robot controller itself. The gravity compensation for the arm and the robot needs to be active during the entire therapy session. The gravity compensation control signal is split into feedforward and feedback parts

$$F_g(t_k) = F_{g_{ff}}(t_k) + F_{g_{fb}}(t_k)$$

The feedforward part is always active. The feedback controller is only activated during the controlled movements (i.e. when the trajectory or target pose is specified) because of the need for a reference signal obtained from the optimal trajectory. When the patient's hand position is lower than the optimal position, a supporting force is produced by the drives and ropes suspended from the ceiling and attached to subject's lower and upper arm.

$$F_{g_{fb}}(t_k) = \begin{cases} k_{p_g}\left(p_{r_z}(t_k) - p_{h_z}(t_k)\right) - k_{v_g} v_{h_z} & \text{if } p_{r_z}(t_k) > p_{h_z}(t_k) \\ 0 & \text{if } p_{r_z}(t_k) \leq p_{h_z}(t_k) \end{cases}$$

Parameters k_{pg} and k_{vg} are the stiffness and the damping values for the feedback controller of the gravity support, p_{rz} is the required vertical position of the hand, p_{hz} is the actual position of the hand and v_{hz} is the vertical velocity of the hand. The feedforward compensation is then adapted in a feedback loop based on the calculated feedback contribution and a simple proportional gain.

$$F_{gff}(t_k) = (1 - \eta_g)\, F_{gff}(t_{k-1}) + k_{g_0} F_{gfb}(t_k)$$

A decrease of the arm weight compensation is introduced through *forgetting* in order to reduce the active support if the patient performs well, i.e. F_{gfb} close to zero. Due to the redundant nature of the human arm it is necessary to split the support force into three components, supporting the upper arm, the lower arm and the wrist, respectively. This force is split based on human anthropometric parameters.

2.5.4 Speech recognition

Analysis of the subject's speech is performed using the commercially available Dragon NaturallySpeaking 9.0 (Professional version). After the software has been trained on a few volunteers, it can recognize a limited number of commands with only a small amount of retraining for each new healthy subject. The software can be programmed to not only directly convert the spoken words to text, but to also input commands into different windows (including Matlab) or even perform advanced scripts. Problems may arise during work with patients, as some (i. e. stroke patients) may have speech impairments. In this case, the speech recognition system will need to be trained more extensively for each patient. In extreme cases, a patient may not be able to use the speech recognition component at all.

3 Real-time sensing of psychophysiological state

3.1 Introduction to the goals of measurements of user's psycho-physiological state

The term psychophysiology refers to the measurement of physiological phenomena as they relate to behaviour in the broadest sense [Andreassi, 2000]. A basic assumption in psychophysiology is that behavioural, cognitive, emotional and social phenomena all have concomitant physiological processes [Hugdahl, 1995]. By measuring these physiological processes, it is possible to obtain an objective measure of the subject's psychological state.
In the scope of the MIMICS project, measuring a subject's psychophysiological state would allow the system to determine how the subject is responding to the virtual environment and the therapy regime. The system can then modify the scenario in order to bring the subject into a desired state. For instance, the system can increase or decrease the difficulty level of a workout depending on whether the subject appears bored or stressed.

3.2 Literature review

Table 1 contains a list of key articles published in the peer-reviewed journals Psychophysiology and the International Journal of Psychophysiology during the last five years. In addition, it contains several fundamental articles about signal acquisition, signal interpretation and related fields.

Table 1: Psychophysiology-related articles

signal domain	parameter	Title (Author, Year)	remarks
electrodermal activity (EDA)	tonic skin conductance level	Publication Recommendations for Electrodermal Measurements (Fowles, 1981)	recommended reading as far as EDA is concerned
		Affective and physiological responses to environmental noises and music (Gomez, 2004)	sounds
		Using Noninvasive Wearable Computers to Recognize Human Emotions from Physiological Signals (Lisetti, 2004)	identifying emotions; contains list of other literature
		Cardiovascular, electrodermal, and respiratory response patterns to fear- and sadness-inducing films (Kreibig, 2007)	response to films; contains list of other literature
		Autonomic specificity of discrete emotion and dimensions of affective space: a multivariate approach (Christie, 2004)	response to films; arousal-valence space

signal domain	parameter	Title (Author, Year)	remarks
		Using psychophysiological measures to measure user experience with entertainment technologies (Mandryk, 2006)	playing computer games, correlation with emotions
		A Continuous and Objective Evaluation of Emotional Experience with Interactive Play Environments (Mandryk, 2006)	fuzzy system for identifying emotions
		Physiological Measures of Presence in Virtual Environments (Meehan, 2001)	virtual reality, presence
		An Investigation into Physiological Responses in Virtual Environments: An Objective Measurement of Presence (Wiederhold, 2001)	virtual reality, presence
		Mechanisms of Virtual Reality Exposure Therapy: The Role of the Behavioural Activation and Inhibition Systems (Wilhelm, 2007)	virtual reality
		Using physiological measures for emotional assessment: a computer-aided tool for cognitive and behavioural therapy (Herbelin, 2004)	virtual reality, arousal-valence space
		A User Model of Psycho-physiological Measure of Emotion (Villon, 2007)	various stimuli, emotion recognition (fairly brief)
		Effects of effort and distress coping processes on psychophysiological and psychological stress responses (Suzuki, 2003)	differences between ways of coping with stress
		Emotion representation and physiology assignments in digital systems (Peter, 2006)	long and informative article about the problems of modelling psychological states
	number of nonspecific SCRs	Publication Recommendations for Electrodermal Measurements (Fowles, 1981)	required reading as far as EDA is concerned
		Combining Skin Conductance and Heart Rate Variability for Adaptive Automation During Simulated IFR Flight (Boucsein, 2007)	using HR, HRV and EDA to create an adaptive VR system
		Predicting autonomic reactivity to public speaking: don't get fixed on self-report data! (Schwerdtfeger, 2003)	public speaking task
		Gender differences in cardiovascular and electrodermal responses to public speaking task: the role of anxiety and mood states (Carrillo, 2001)	public speaking task

signal domain	parameter	Title (Author, Year)	remarks
		Cardiovascular, electrodermal, and respiratory response patterns to fear- and sadness-inducing films (Kreibig, 2007)	response to films; contains list of other literature
		A User Model of Psycho-physiological Measure of Emotion (Villon, 2007)	various stimuli, emotion recognition (fairly brief)
		A comparison of psychophysiological and self-report measures of BAS and BIS activation (Brenner, 2005)	different levels of reward and frustration
		Respiratory sinus arrhythmia as an index of emotional response in young adults (Frazier, 2004)	arousal-valence space
	nonspecific SCR amplitude	Publication Recommendations for Electrodermal Measurements (Fowles, 1981)	required reading as far as EDA is concerned
		Combining Skin Conductance and Heart Rate Variability for Adaptive Automation During Simulated IFR Flight (Boucsein, 2007)	using HR, HRV and EDA to create an adaptive VR system
		Gender differences in cardiovascular and electrodermal responses to public speaking task: the role of anxiety and mood states (Carrillo, 2001)	public speaking task
		Cardiovascular, electrodermal, and respiratory response patterns to fear- and sadness-inducing films (Kreibig, 2007)	response to films; contains list of other literature
		A User Model of Psycho-physiological Measure of Emotion (Villon, 2007)	various stimuli, emotion recognition (fairly brief)
	specific SCR	Publication Recommendations for Electrodermal Measurements (Fowles, 1981)	required reading as far as EDA is concerned
		Identifying Structural Features of Radio: Orienting and Memory for radio Messages (Potter, 1997)	listening to sounds
		The Psychophysiology of James Bond: Phasic Emotional Responses to Violent Video Game Events (Ravaja, 2007)	playing video games
		Using psychophysiological measures to measure user experience with entertainment technologies (Mandryk, 2006)	playing computer games, correlation with emotions
		Psychophysiological responses to appraisal dimensions in a computer game (van Reekum, 2004)	computer games, correlation with emotions

signal domain	parameter	Title (Author, Year)	remarks
		Analysis of Physiological Responses to a Social Situation in an Immersive Virtual Environment (Slater, 2003)	virtual reality
		The skin conductance orienting response to semantic stimuli: Significance can be independent of arousal (Dindo, 2008)	response to words
		Heart rate and skin conductance analysis of antecendents and consequences of decision making (Crone, 2004)	gambling
electrocardiogram	heart rate	Combining Skin Conductance and Heart Rate Variability for Adaptive Automation During Simulated IFR Flight (Boucsein, 2007)	using HR, HRV and EDA to create an adaptive VR system
		Predicting autonomic reactivity to public speaking: don't get fixed on self-report data! (Schwerdtfeger, 2003)	public speaking task
		Gender differences in cardiovascular and electrodermal responses to public speaking task: the role of anxiety and mood states (Carrillo, 2001)	public speaking task
		Respiratory sinus arrhythmia, emotion, and emotion regulation during social interaction (Butler, 2006)	upsetting films and discussion
		Affective and physiological responses to environmental noises and music (Gomez, 2004)	sounds
		Identifying Structural Features of Radio: Orienting and Memory for radio Messages (Potter, 1997)	listening to sounds
		Using Noninvasive Wearable Computers to Recognize Human Emotions from Physiological Signals (Lisetti, 2004)	identifying emotions; contains list of other literature
		Cardiovascular, electrodermal, and respiratory response patterns to fear- and sadness-inducing films (Kreibig, 2007)	response to films; contains list of other literature
		Autonomic specificity of discrete emotion and dimensions of affective space: a multivariate approach (Christie, 2004)	response to films; arousal-valence space
		Using psychophysiological measures to measure user experience with entertainment technologies (Mandryk, 2006)	playing computer games, correlation with emotions

signal domain	parameter	Title (Author, Year)	remarks
		A Continuous and Objective Evaluation of Emotional Experience with Interactive Play Environments (Mandryk, 2006)	fuzzy system for identifying emotions
		Analysis of Physiological Responses to a Social Situation in an Immersive Virtual Environment (Slater, 2003)	virtual reality
		Physiological Measures of Presence in Virtual Environments (Meehan, 2001)	virtual reality, presence
		An Investigation into Physiological Responses in Virtual Environments: An Objective Measurement of Presence (Wiederhold, 2001)	virtual reality, presence
		Mechanisms of Virtual Reality Exposure Therapy: The Role of the Behavioural Activation and Behavioural Inhibition Systems (Wilhelm, 2007)	virtual reality
		The effects of the spontaneous presence of a spouse/partner and others on cardiovascular reactions to an acute psychological challenge (Phillips, 2006)	presence of others
		A User Model of Psycho-physiological Measure of Emotion (Villon, 2007)	various stimuli, emotion recognition (fairly brief)
		Heart rate and skin conductance analysis of antecendents and consequences of decision making (Crone, 2004)	gambling
		Effects of effort and distress coping processes on psychophysiological and psychological stress responses (Suzuki, 2003)	differences between ways of coping with stress
		Relative effects of harassment, frustration, and task characteristics on cardiovascular reactivity (Leon, 2003)	response to frustration during task
		Emotion representation and physiology assignments in digital systems (Peter, 2006)	long and informative article about the problems of modelling psychological states
	HRV (time domain)	Heart Rate Variability: Standards of measurement, physiological interpretation, and clinical use (1996)	required reading as far as HRV is concerned
		Heart Rate Variability: Origins, methods and interpretive caveats (Berntson, 1997)	extension of above

signal domain	parameter	Title (Author, Year)	remarks
		Combining Skin Conductance and Heart Rate Variability for Adaptive Automation During Simulated IFR Flight (Boucsein, 2007)	using HR, HRV and EDA to create an adaptive VR system
		Autonomic specificity of discrete emotion and dimensions of affective space: a multivariate approach (Christie, 2004)	response to films; arousal-valence space
		Analysis of Physiological Responses to a Social Situation in an Immersive Virtual Environment (Slater, 2003)	virtual reality
	HRV (frequency domain)	Heart Rate Variability: Standards of measurement, physiological interpretation, and clinical use (1996)	required reading as far as HRV is concerned
		Heart Rate Variability: Origins, methods and interpretive caveats (Berntson, 1997)	extension of above
		Respiratory sinus arrhythmia: Autonomic origins, physiological mechanisms, and psychophysiological implications (Berntson, 1993)	mechanisms and interpretation of RSA
		Respiratory sinus arrhythmia, emotion, and emotion regulation during social interaction (Butler, 2006)	upsetting films and discussion
		Presence-related Influences of a Small Talking Facial Image on Psychophysiological Measures of Emotion and Attention (Ravaja)	watching talking faces
		Cardiovascular, electrodermal, and respiratory response patterns to fear- and sadness-inducing films (Kreibig, 2007)	response to films; contains list of other literature
		Analysis of Physiological Responses to a Social Situation in an Immersive Virtual Environment (Slater, 2003)	virtual reality
		A User Model of Psycho-physiological Measure of Emotion (Villon, 2007)	various stimuli, emotion recognition (fairly brief)
		A comparison of psychophysiological and self-report measures of BAS and BIS activation (Brenner, 2005)	different levels of reward and frustration
		Respiratory sinus arrhythmia as an index of emotional response in young adults (Frazier, 2004)	arousal-valence space
		Relative effects of harassment, frustration, and task characteristics on cardiovascular reactivity (Leon, 2003)	response to frustration during task

signal domain	parameter	Title (Author, Year)	remarks
finger pulse	finger pulse volume and rate	Gender differences in cardiovascular and electrodermal responses to public speaking task: the role of anxiety and mood states (Carrillo, 2001)	public speaking task
		Cardiovascular, electrodermal, and respiratory response patterns to fear- and sadness-inducing films (Kreibig, 2007)	response to films; contains list of other literature
		Using physiological measures for emotional assessment: a computer-aided tool for cognitive and behavioural therapy (Herbelin, 2004)	virtual reality, arousal-valence space
		Relative effects of harassment, frustration, and task characteristics on cardiovascular reactivity (Leon, 2003)	response to frustration during task
	pulse transit time	Psychophysiological responses to appraisal dimensions in a computer game (van Reekum, 2004)	computer games, correlation with emotions
respiration	respiration rate	Respiratory sinus arrhythmia, emotion, and emotion regulation during social interaction (Butler, 2006)	upsetting films and discussion
		Affective and physiological responses to environmental noises and music (Gomez, 2004)	listening to sounds
		Cardiovascular, electrodermal, and respiratory response patterns to fear- and sadness-inducing films (Kreibig, 2007)	response to films; contains list of other literature
		Using psychophysiological measures to measure user experience with entertainment technologies (Mandryk, 2006)	playing computer games, correlation with emotions
		Using physiological measures for emotional assessment: a computer-aided tool for cognitive and behavioural therapy (Herbelin, 2004)	virtual reality, arousal-valence space
		Relative effects of harassment, frustration, and task characteristics on cardiovascular reactivity (Leon, 2003)	response to frustration during task
	volume	Respiratory sinus arrhythmia, emotion, and emotion regulation during social interaction (Butler, 2006)	upsetting films and discussion
		Affective and physiological responses to environmental noises and music (Gomez, 2004)	listening to sounds

signal domain	parameter	Title (Author, Year)	remarks
		Cardiovascular, electrodermal, and respiratory response patterns to fear- and sadness-inducing films (Kreibig, 2007)	response to films; contains list of other literature
		Using psychophysiological measures to measure user experience with entertainment technologies (Mandryk, 2006)	playing computer games, correlation with emotions
		Cardiorespiratory response under combined psychological and exercise stress (Rousselle, 1995)	exercise andcognition
facial electromyography	corrugator supercilii	Guidelines for Human Electromyographic Research (Fridlund, 1986)	required reading
		Presence-related Influences of a Small Talking Facial Image on Psychophysiological Measures of Emotion and Attention (Ravaja)	watching talking faces
		The Psychophysiology of James Bond: Phasic Emotional Responses to Violent Video Game Events (Ravaja, 2007)	playing video games
		A Continuous and Objective Evaluation of Emotional Experience with Interactive Play Environments (Mandryk, 2006)	fuzzy system for identifying emotions
		Electromyographic responses to static and dynamic avatar emotional facial expressions (Weyers, 2006)	virtual reality
	zygomaticus major	Guidelines for Human Electromyographic Research (Fridlund, 1986)	required reading
		Presence-related Influences of a Small Talking Facial Image on Psychophysiological Measures of Emotion and Attention (Ravaja)	watching talking faces
		The Psychophysiology of James Bond: Phasic Emotional Responses to Violent Video Game Events (Ravaja, 2007)	playing video games
		Using psychophysiological measures to measure user experience with entertainment technologies (Mandryk, 2006)	playing computer games, correlation with emotions
		A Continuous and Objective Evaluation of Emotional Experience with Interactive Play Environments (Mandryk, 2006)	fuzzy system for identifying emotions

signal domain	parameter	Title (Author, Year)	remarks
		Electromyographic responses to static and dynamic avatar emotional facial expressions (Weyers, 2006)	virtual reality
	orbicularis oculi	Guidelines for Human Electromyographic Research (Fridlund, 1986)	required reading
		The Psychophysiology of James Bond: Phasic Emotional Responses to Violent Video Game Events (Ravaja, 2007)	playing video games
		Event-related potentials, cognition, and behavior: a biological approach (Kotchoubey B, 2006)	
temperature	finger temperature	Using Noninvasive Wearable Computers to Recognize Human Emotions from Physiological Signals (Lisetti, 2004)	identifying emotions; contains list of other literature
		Cardiovascular, electrodermal, and respiratory response patterns to fear- and sadness-inducing films (Kreibig, 2007)	response to films; contains list of other literature
		Fingertip temperature as an indicator for sympathetic responses (Kistler, 1997)	various stimuli
		Psychophysiological responses to appraisal dimensions in a computer game (van Reekum, 2004)	computer games, correlation with emotions
		Physiological Measures of Presence in Virtual Environments (Meehan, 2001)	virtual reality, presence
		Using physiological measures for emotional assessment: a computer-aided tool for cognitive and behavioural therapy (Herbelin, 2004)	virtual reality, arousal-valence space
		Emotion representation and physiology assignments in digital systems (Peter, 2006)	long and informative article about the problems of modelling psychological states
blood pressure	blood pressure	Cardiovascular, electrodermal, and respiratory response patterns to fear- and sadness-inducing films (Kreibig, 2007)	response to films; contains list of other literature
		Autonomic specificity of discrete emotion and dimensions of affective space: a multivariate approach (Christie, 2004)	response to films; arousal-valence space

signal domain	parameter	Title (Author, Year)	remarks
		The effects of the spontaneous presence of a spouse/partner and others on cardiovascular reactions to an acute psychological challenge (Phillips, 2006)	presence of others
		Effects of effort and distress coping processes on psychophysiological and psychological stress responses (Suzuki, 2003)	differences between ways of coping with stress
		Relative effects of harassment, frustration, and task characteristics on cardiovascular reactivity (Leon, 2003)	response to frustration during task
getting psychological states from physiological signals		Emotion representation and physiology assignments in digital systems (Peter, 2006)	long and informative article about the problems of modelling psychological states
		Autonomic specificity of discrete emotion and dimensions of affective space: a multivariate approach (Christie, 2004)	response to films; arousal-valence space
		Using psychophysiological measures to measure user experience with entertainment technologies (Mandryk, 2006)	playing computer games, correlation with emotions
		A Continuous and Objective Evaluation of Emotional Experience with Interactive Play Environments (Mandryk, 2006)	fuzzy system for identifying emotions
		Using physiological measures for emotional assessment: a computer-aided tool for cognitive and behavioural therapy (Herbelin, 2004)	virtual reality, arousal-valence space
		A User Model of Psycho-physiological Measure of Emotion (Villon, 2007)	various stimuli, emotion recognition (fairly brief)
		Psychophysiological responses to appraisal dimensions in a computer game (van Reekum, 2004)	computer games, correlation with emotions
		Combining Skin Conductance and Heart Rate Variability for Adaptive Automation During Simulated IFR Flight (Boucsein, 2007)	using HR, HRV and EDA to create an adaptive VR system
		Using Noninvasive Wearable Computers to Recognize Human Emotions from Physiological Signals (Lisetti, 2004)	identifying emotions; contains list of other literature

signal domain	parameter	Title (Author, Year)	remarks
reviews of literature		Methods and Models for the Psychophysiology of Emotion, Arousal and Personality (Boucsein and Backs, 2008)	solely a literature review
		Psychophysiology in Digital Human Modeling (Backs and Boucsein, 2008)	solely a literature review
		Aroused and Immersed: The Psychophysiology of Presence (Dillon, 2000)	solely a literature review
		Cardiovascular, electrodermal, and respiratory response patterns to fear- and sadness-inducing films (Kreibig, 2007)	response to films; contains list of other literature
		Using Noninvasive Wearable Computers to Recognize Human Emotions from Physiological Signals (Lisetti, 2004)	identifying emotions; contains list of other literature

3.3 Electrodermal response (Galvanic skin response)

3.3.1 Physiological basis

Electrodermal responses are changes in the electrical properties of a person's skin caused by an interaction between environmental events and the individual's psychological state. The superficial layer of the skin, the epidermis, ordinarily has a high electrical resistance due to a thick layer of dead cells. However, it is penetrated by sweat ducts from underlying cells. As these ducts fill, a relatively good conductor emerges, and many low-resistance parallel pathways result. A further increase in conductance results from the hydration of the skin due to the flow of sweat across the duct walls. As a consequence the effective skin conductance can vary greatly. These changes are especially pronounced in the palmar and plantar regions. While the epidermis there is very thick, sweat glands are also unusually dense. It should be noted that the filling of ducts with sweat can take place before any (observable) release of sweat onto the skin surface and/or noticeable diffusion into the skin. [Malvimuo, J. and Plonsey, R., 1995]

3.3.2 Measurement

There are two different approaches to measuring the electrodermal response. The first involves the measurement of resistance or conductance between two electrodes placed in the palmar region. The second involves detecting voltage changes between these two electrodes; these potential waveforms appear to be similar to the passive resistance changes, though their interpretation is less well understood. The first type of measurement is referred to as exosomatic, since the current on which the measurement is based is introduced from the outside. The second type is called endosomatic, since the source of voltage is internal. It is generally not recommended, as the biphasic nature of skin potential responses makes amplitude measures difficult to interpret, and the sensitivity of skin potential levels to hydration effects is significant. [Malvimuo, J. and Plonsey, R., 1995] For this reason, only the first method will be discussed.

Electrodermal responses are best measured at palmar sites, and skin conductance is recommended over skin resistance. The most important article on the subject of measuring electrodermal activity is »Publication recommendations for electrodermal measurements« [Fowles, 1981]. Most articles written on the subject of electrodermal activity follow the measurement guidelines presented therein. Some of the most important findings from the article are presented below.

For measuring skin conductance, electrodes must show a minimal bias potential and not polarize upon the passage of a current. Silver-silver chloride (Ag-AgCl) electrodes have been found to be most satisfactory. They should be recessed from the skin and require the use of a suitable electrode paste that contains NaCl at the concentration of sweat (approximately 0.3%). A contact area of 1.0 cm2 is recommended. If an area this large cannot be achieved, the maximal area permitted by the recording site is recommended. Measurements should be recorded with bipolar placements – with both electrodes on active sites. Several suitable sites are found on the palms: the thenar and hypothenar eminences and the medial and distal phalanges of the fingers (Figure 20). Bipolar placements should be kept on the same hand to avoid ECG artifacts.

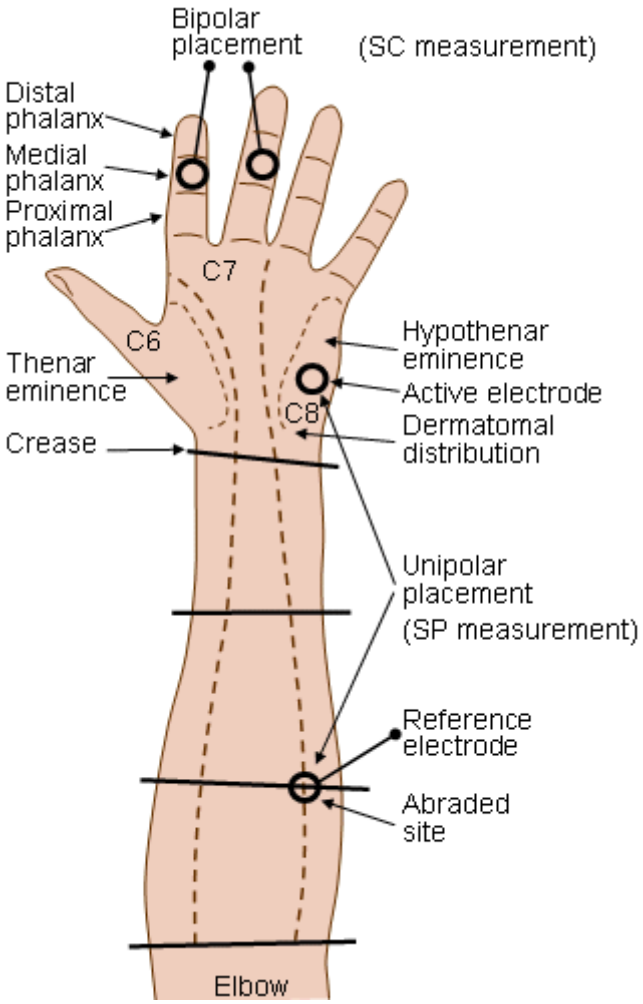

Figure 20 Electrode placement sites for skin conductance and skin potential measurement [Malvimuo, J. and Plonsey, R., 1995]

In most studies, measurements are taken from palmar sites. If this is not possible (such as when both hands must be used to perform a task), recordings may be taken from the plantar surface of the feet. The most suitable site is on the medial side of the foot over the abductor hallucis muscle adjacent to the plantar surface and midway between the first phalanx and a point directly beneath the ankle.

Skin conductance measurements are obtained by measuring the current flow through the skin in response to a constant applied voltage. For bipolar recordings, 0.5 volt is recommended. It is essential that this applied voltage be constant.

3.3.3 Significant Relevant variables in the signal

Two types of skin conductance are characterized, tonic and phasic. Tonic skin conductance is the baseline level of skin conductance, in the absence of any particular discrete environmental event, and is generally referred to as Skin Conductance Level (SCL). Each person has a different SCL, with typical tonic levels ranging from 10 to 50 μS. Tonic skin conductance levels vary over time in individuals depending on psychological state and autonomic regulation.

Phasic skin conductance is the type that changes when events take place. Discrete environmental stimuli evoke time-related changes in skin conductance. These are generally referred to as Skin Conductance Responses (SCRs). SCRs are increases in the conductance of the skin followed by a return to the tonic or baseline level of skin conductance (Figure 21). These phasic changes are often simply called GSRs (galvanic skin responses), but this is considered to be an outdated term.

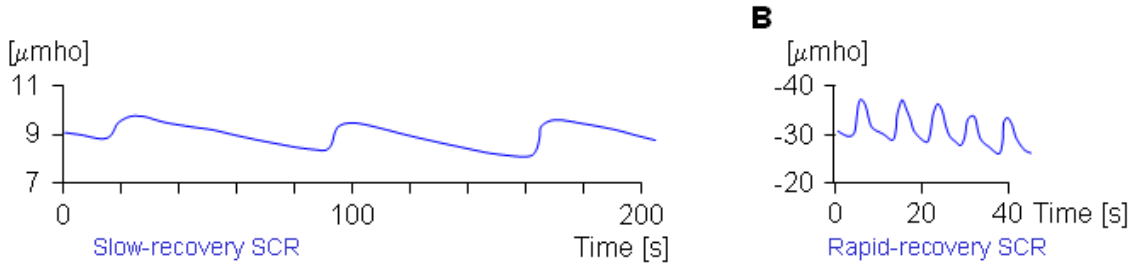

Figure 21 Typical skin conductance responses [Malvimuo, J. and Plonsey, R., 1995]

The parameters of event-related SCRs that are usually quantified are amplitude, latency, rise time and half-recovery time. In addition, individuals show spontaneous SCRs to varying degrees even in the absence of specific events. The frequency of these nonspecific SCRs is also often measured. Generally, all changes in skin conductance from baseline that exceed a certain threshold (usually 0.05 μS) are classified as nonspecific SCRs.

3.3.4 Relation to psychological state

Electrodermal activity is a measure solely of the activity of the sympathetic autonomic nervous system (ANS). Amplitudes of SCRs reflect the amount of affective or emotional arousal elicited by a stimulus or situation. Orienting and habituation can be easily seen in SCR amplitudes [Boucsein & Becks, 2008]. Both amplitude and half-recovery time have been demonstrated to be sensitive for certain aspects of central information processing and may be used as indicators of mental activity. The frequency of nonspecific SCRs is a valid indicator of emotional strain and has shown specific sensitivity during human-computer interaction. [Boucsein & Becks, 2008]

3.4 Heart rate and heart period

3.4.1 Measurement

Two methods of accurately measuring heart rate are widespread: via blood pressure measurement and via electrocardiography (ECG). Blood pressure is not suitable for continuous measurement, so most psychophysiological studies derive heart rate from the ECG. The ECG records the electrical current in the heart in the form of a continuous graph. The so-called QRS complex that represents ventricular depolarization can be detected with different detection algorithms. However, the ECG is sensitive to noise and especially motion artifacts. Most psychophysiological measurements have focused on situations with little motion. The ECG can be recorded from the limbs or the chest. For low-motion situations such as typing or writing, motion artifacts for limb-recorded ECG are generally weak enough to allow QRS detection. A sampling frequency of at least 500 Hz is recommended.

3.4.2 Relevant variables in the signal

The heart rate (HR) represents the number of heartbeats per minute. The information it contains is equivalent to the information contained in the heart period (HP), which represents the time between two heartbeats. Here, we must differentiate between the so-called RR interval (the time between two adjacent heartbeats) and the NN interval (the time between two adjacent normal heartbeats). Most psychophysiological studies evaluate the ECG signal and remove abnormal heartbeats.

HR and HP can be used as psychophysiological indicators on their own. Additionally, it is possible to calculate simple time-domain variables such as average HR and HP, the difference between the longest and shortest heart period during a particular interval etc. For series of HR or HP measurements recorded over longer periods (traditionally 24 hours), more complex statistical time-domain measures can be calculated. However, our studies are unlikely to involve long-term HR measurement. A few statistical time-domain variables are used for short-term measurements (traditionally 5 minutes). They include the standard deviation of the NN interval (i.e. the square root of variance), the square root of the mean squared differences of successive NN intervals and others. [Task Force, 1996]

Heart rate variability (HRV) is more often analyzed in detail using frequency-domain methods (usually using interpolation and a resolution of 4 Hz). These methods require HR and HP to be converted into instantaneous time series. Power spectral density (PSD) provides information of how power is distributed as a function of frequency. Methods for the estimation of PSD may be generally classified as non-parametric and parametric. In most instances, both methods provide similar results, and psychophysiological studies usually use Welch's method with a Hanning window and 50% overlap between intervals. Frequency-domain methods are not recommended for recordings shorter than 2 to 5 minutes. [Task Force, 1996]

Two relevant spectral components are distinguished in a spectrum calculated from short-term recordings of 2 to 5 minutes: the low frequency (LF, between 0.04 and 0.15 Hz) and high frequency (HF, between 0.15 and 0.4 Hz) components. Higher-frequency activity is not used for psychophysiological research. Very low frequency activity (VLF, below 0.04 Hz) is generally used in 24-hour heart rate recordings and is therefore not relevant to our goals. Vagal (parasympathetic) activity is the major

contributor to the HF component, while disagreement exists in respect to the LF component. Some studies suggest that it is a marker of sympathetic modulations while others view it as a reflection of both sympathetic and vagal activity. The distribution of the power and the central frequency of LF and HF are not fixed but may vary in relation to changes in autonomic modulations of the heart period. VLF assessed from short-term recordings is a dubious measure and should be avoided. Total LF power and total HF power are usually calculated in absolute values of power, but may also be measured in normalized units, which represent the relative value of each power component in proportion to the sum of the two components. Representation in normalized units tends to minimize the effects of changes in total power and emphasizes the controlled and balanced behavior of branches of the ANS. One of the most important estimates of heart rate variability obtained from the frequency domain is the total LF power divided by the total HF power (the LF/HF ratio). [Task Force, 1996]

For psychophysiology, an important spectral component of HRV is respiratory sinus arrhythmia (RSA). RSA refers to rhythmic fluctuations in heart rate associated with respiration. All studies agree that the lower bound for respiration-related activity in the HRV power spectrum is 0.15 Hz. However, not all studies agree on the upper bound, so the frequency band of respiration-related activity has been defined variously as 0.15 Hz – 0.4 Hz, 0.15 Hz – 0.5 Hz, and the frequency band above 0.15 Hz. This is about equal to the HF component mentioned above RSA is computed by summing power spectral densities over this frequency band. If respiration is monitored, RSA can be assessed as the difference between the shortest heart period found during inspiration and the longest heart period found during expiration.

Another measure of cardiovascular activity is the pulse transfer time. To estimate it, two separate measurements are required: the ECG and the finger pulse signal. It is calculated for a particular heartbeat as the time between the R-wave peak in the ECG and its corresponding peak in the finger pulse. However, it is very difficult to estimate accurately if the subject is moving and will therefore not be used.

3.4.3 Relation to psychological state

The heart is innervated by both sympathetic and parasympathetic fibers from the ANS. Heart rate is used as an indicator of physical as well as mental load [Mulder et al., 2000]. Although tonic HR changes may indicate the need for energy supply in response preparation, phasic HR patterns can be used to determine stimulus-directed central processing activity. Orienting responses consist of a HR decrease, followed by increase, while defensive or startle responses lead to an immediate HR increase [Turpin, 1985]. HR is larger for fear and anger than for happiness and disgust [Cacioppo et al., 2000]. Time pressure during human-computer interaction can also increase HR [Boucsein, 2000]. HRV decreases with mental workload in complex task environments [Veltman & Gaillard, 1998]. RSA has been suggested as a measure of controlled attention [Laarni et al., 2003]. Some authors [Beauchaine, 2001] also suggest that high levels of resting RSA are indicative of physiological flexibility, while low levels of resting RSA in adults have been associated with a wide range of psychopathologies such as excessive rigidity [Thayer & Lane, 2000].

3.5 Blood pressure

3.5.1 Measurement

Arterial pressure can be measured from the arm, wrist or finger using cuffs. These cuffs are extremely sensitive to motion and are generally unsuitable for long-term continuous measurement, which may involve an unsystematic drift over time. Many psychophysiological studies use commercially available blood pressure monitoring devices such as the Finapres (for measurement of blood pressure from the left middle finger), the Vasotrac (from the radial artery of the wrist) or the Dinamap 1846SX (from the upper arm). In all cases, the arm to which the device is attached must remain still.

3.5.2 Relevant variables in the signal

The two most significant variables are systolic and diastolic blood pressure – the highest and lowest blood pressures during a beat. Another relevant variable is the mean arterial pressure, defined as the mean blood pressure over a beat. These three variables can be tracked beat-to-beat or as averages over a longer time period.

3.5.3 Relation to psychological state

Blood pressure is frequently used as an indicator of physical or mental stress [Boucsein & Becks, 2008]. Increases in systolic BP appear as long-term consequences of highly demanding mental tasks [Rose & Fogg, 1993], but also in other work (such as data entry) if time pressure is a factor [Boucsein, 2000]. Diastolic BP was found to be higher when viewing angry compared to happy, sad, fearful or relaxed faces [Schwartz et al., 1981].

3.6 Peripheral skin temperature

3.6.1 Measurement

Peripheral skin temperature is commonly measured from the palmar surface of the distal phalanx of the fifth finger using a thermistor.

3.6.2 Relevant variables in the signal

Skin temperature by itself is the only variable regularly used in psychophysiological studies. As skin temperature is a slow-changing signal, it has been suggested that its first derivative may be a better event-related indicator since it changes more quickly [van Reekum, 2004]. The first derivative is averaged over an interval of a few seconds to remove noise. However, studies of temperature slope are currently limited.

3.6.3 Relation to psychological state

Skin temperature changes slowly and is therefore unsuitable for evaluation of short-term changes. It increases during physical and environmental strain [Romet & Frim, 1987]. It also increases while viewing happy film clips [Rimm-Kaufmann & Kagan, 1996], but decreases during emotional strain in computer work [Ohsuga et al., 2001], threatening personal questions and tense situations such as car driving [Min et al.,

2002]. Skin temperature slopes behave differently in conducive and obstructive events during a computer game [Van Reekum et al., 2004].

3.7 Respiration

3.7.1 Measurement

Respiration can be measured using a respiratory plethysmograph (an instrument for measuring changes in volume within an organ). Two bands are placed around the body: one high on the chest above the breasts (thoracic respiration), the other below the navel and above the pants (abdominal respiration). Many psychophysiological studies use only thoracic respiration. The signals are converted to lung volume change using data from a fixed volume bag calibration procedure.

Though chest bands are accurate, they are sensitive to motion artifacts. If motion is required during the study, respiration is better measured using a thermistor in the nostrils. The thermistor measures temperature changes caused by the subject inhaling and exhaling air.

Ergospirometry can be used to determine respiration more precisely. Additionally to the ventilatory parameters metabolic parameters like oxygen consumption and carbon dioxide production, can be assessed. Standard ergospirometry systems analyze these values breath by breath. Therefore these systems uses bidirectional digital turbines which measures the air passing through. Oxygen and carbon dioxide analyzers determine the gas concentrations.

3.7.2 Relevant variables in the signal

If measuring respiration using a thermistor attached to the nose, the only variable that can be measured is respiration rate (the number of breaths per minute). A respiratory plethysmograph allows measurement of tidal volume (the amount of air breathed in or out during normal respiration) and minute ventilation (the product of respiration rate and tidal volume). These are the most frequent variables used in psychophysiological research. Others include inspiratory flow rate (in ml/s), duty cycle (inspiratory to whole cycle ratio) and tidal volume variability (root mean square successive difference of tidal volumes).

3.7.3 Relation to psychological state

Respiration rate is most frequently used to control for respiratory artifacts in various other psychophysiological measures. In addition, respiration rate, inspiratory flow and duty cycle are associated with emotional arousal, but may also be influenced by the affective valence of the stimuli. Respiration becomes unstable during periods of boredom in computer work [Ohsuga et al., 2001], and tidal volume variability has been found to be related to panic diagnosis and acute anxiety. When playing a computer game, expert players were found to have a higher mean respiration rate than novice or semi-experienced players, and the respiration rate for most players was inversely correlated with frustration [Mandryk et al., 2006]. Several studies found that respiration rate is correlated with fear [Kreibig et al., 2007]. Respiration tends to synchronize to musical rhythms, so respiratory parameters are different

when listening to music than when listening to other noises [Gomez and Danuser, 2004].

3.8 Facial electromyography

3.8.1 Measurement

The electrical activity of three facial muscles has been measured in psychophysiological studies: the corrugator supercilii, the zygomaticus major and the orbicularis oculi. Recommendations for psychophysiological EMG measurement can be found in Guidelines for human electromyographic research [Fridlund & Cacioppo, 1986]. The most important guidelines are listed in the following paragraph.

EMG researchers in psychophysiology typically use electrodes with 0.25 cm Ag-AgCl detection surfaces for facial measurements. A 1-cm inter-electrode spacing is recommended. After the skin is cleaned, electrodes are placed in a bipolar configuration (see Figure 22 for a diagram of common facial EMG electrode sites). For the corrugator supercilii, one electrode is affixed directly above the brow on an imaginary vertical line that traverses the inner commissure of the eye fissure. The second electrode is positioned 1 cm lateral to, and slightly superior to, the first on the border of the eyebrow. For the zygomaticus major, one electrode is placed midway along an imaginary line joining the cheilion and the preauricular depression (the bony dimple above the posterior edge of the zygomatic arch), and the second electrode is placed 1 cm inferior and medial to the first (ie. toward the mouth) along the same imaginary line. For the orbicularis oculi, electrodes are placed in the inferior orbital portion (which constricts the eye fissure). The first electrode is affixed 1 cm inferior to the outer commissure of the eye fissure while the second is played 1 cm medial to and slightly inferior to the first so that the electrode pair runs parallel to the lower edge of the eyelid. Reduction of the interelectrode resistance is required for weak EMG signals. Generally, if resistance exceeds 10 kiloohms, the skin should be cleaned again and the electrodes reapplied.

Electrical activity in the jaw muscles indicates tension of the jaw. The disadvantage of using surface electrodes is that the signals can be distorted by other jaw activity such as smiling, laughing and talking. Needle electrodes are an alternative to surface electrodes that minimise interference, but are usually not appropriate for psychophysiological studies. Very few psychophysiological studies have measured EMG during physical activity. It is uncertain to what degree sweating may affect EMG measurements.

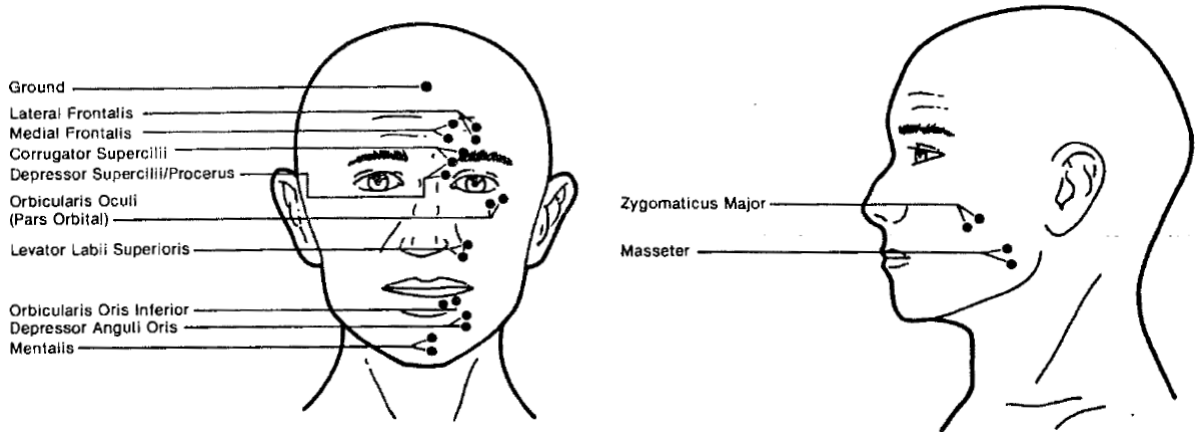

Figure 22: Electrode placement for facial EMG measurement [Fridlund & Cacioppo, 1986]

3.8.2 Relevant variables in the signal

After filtering, the raw EMG signal is rectified and smoothed. Usually, the rectified smoothed EMG signal is used as an indicator of muscle activity.

3.8.3 Relation to psychological state

The corrugator supercilii has been nicknamed the »frown muscle« and the zygomaticus major has been nicknamed the »smile muscle«. EMG activity over the brow (m. corrugator supercilii) is lower and EMG activity over the cheek (m. zygomaticus major) is higher when emotions are positive as opposed to negative [Larsen et al., 2003; Cacioppo et al., 2000; Simons et al., 1999]. EMG activity of the orbicularis oculi is usually correlated with EMG activity of the zygomaticus major, so many psychophysiological studies do not measure activity of the orbicularis oculi.

3.9 Measurement Setup

3.9.1 ECG

ECG electrodes are placed on the body. Though several positions can be used for measurement, UL uses the positioning shown in the g.tec ECG instructions: two electrodes on the thorax, one on the abdomen, and one on the shoulder (Figure 23). ETH positions the electrodes according to the second derivation of Nebh A (anterior). The first electrode is attached to the fourth intercostal space and the second is attached to the apex of the heart on the left side of the midclavicular line. The third electrode is attached to the right collarbone and serves as the ground.

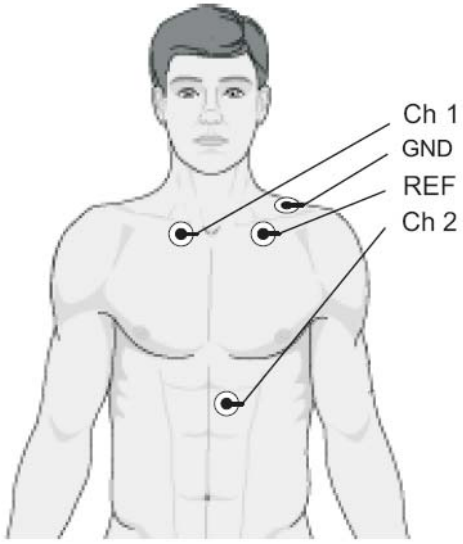

Figure 23: ECG electrode positioning used by UL

3.9.2 Electrodermal response

g.tec's g.GSR sensor is used to measure electrodermal activity. The electrodes are attached to the medial phalanxes of the second and third fingers (as is common in literature) using Velcro straps. UL and ETH uses the same method.

3.9.3 Respiration

The SleepSense Flow Sensor is used to estimate respiration rate. It is placed beneath the nose, with the larger part covering the mouth and the smaller part bent slightly so it does not actually enter the nose. UL and ETH uses the same method.

3.9.4 Blood pressure

Two sensors are attached to two neighbouring fingers of one hand. An additional sensor is mounted around the upper arm. This setup allows continuous recording of blood pressure information.

3.9.5 Skin temperature

Both UL and ETH use g.tec's g.Temp sensor to measure peripheral skin temperature. The sensor is attached to the distal phalanx of the fifth finger, as is common in literature.

3.9.6 Pulse

UL uses g.tec's G.Pulse sensor to measure finger pulse. The sensor is attached to the distal phalanx of the thumb.

3.9.7 Facial EMG

UL measures the activity of two muscles: the corrugator supercilii and the zygomaticus major. Electrodes are placed according to "Guidelines for Human Electromyographic Research" [Fridlund, 1986]. ETH uses facial EMG only to detect eye blinking.

3.9.8 Electroencephalography (EEG)

EEG measurements are taken in order to assess brain activity during walking in the Lokomat. Electrodes are placed according to an international standardized electrode position system (10-20 system [Jasper, 1958]).

3.9.9 EMG of lower leg muscles

EMG of lower leg muscles are measured in the Lokomat because Lokomat provides only biomechanical information on hip and knee joint. To assess additionally the activity of the ankle EMG of tibialis anterior (TA) and gastrocnemius (GM) are measured. The EMG is sampled at 1000 Hz. This signal is only used for offline analyses.

3.9.10 Spirometry

A standard ergospirometry acquisition system is used, and the signals are analysed offline.

3.10 Signal acquisition

3.10.1 Hardware setup (g.tec)

All of the signals are sampled using g.tec's gUSBamp biosignal amplifier. For facial electromyography, a sampling frequency of above 2 kHz is required, so g.tec's built-in 2400-Hz setting is used for all signals. In the absence of facial electromyography, the sampling frequency may be lower if necessary, but no lower than 512 Hz. The bandpass filters built into the g.USBamp interface were not used, as digital filtering can be applied later to extract useful parameters. A block diagram of the hardware setup is shown on Figure 24.

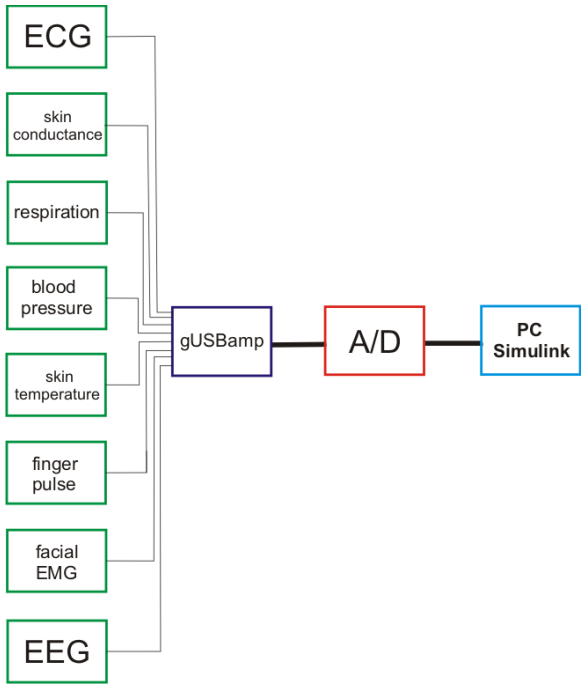

Figure 24: Block diagram of psychophysiological hardware

3.10.2 Software setup (soft real-time Matlab/Simulink platform)

g.tec has provided drivers that allow us to connect the gUSBamp amplifier to a PC using a USB port. Additionally, a Simulink block has been provided that converts the gUSBamp signals to digital form and imports them into Simulink. The block also allows the user to specify sampling rate, frame length, triggering and other options. A screenshot of the Simulink block and its interface is shown on Figure 25.

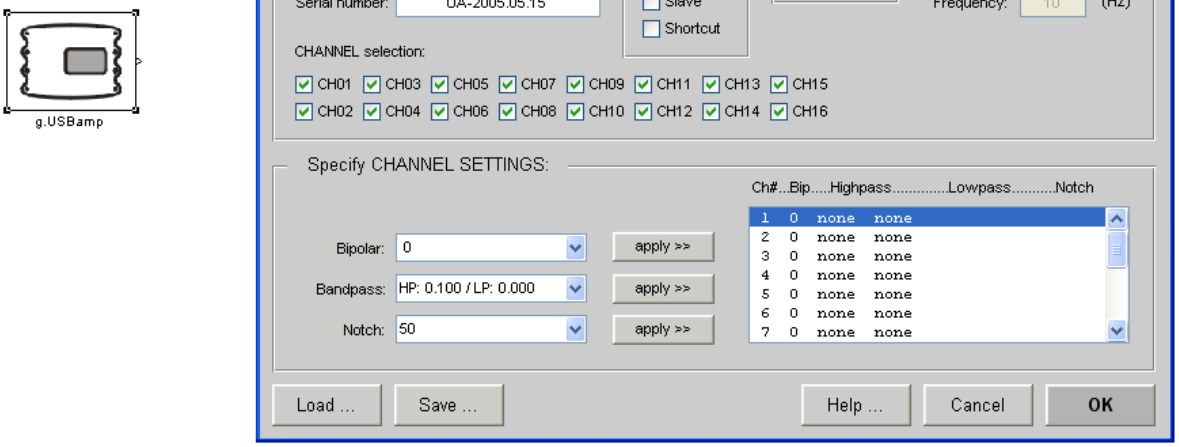

Figure 25: gUSBamp Simulink interface

3.11 Signal Analysis

3.11.1 ECG

The first step in analyzing the ECG is extracting the locations of the QRS complexes. Due to its characteristic shape (Figure 26), the QRS complex serves as the basis for the calculation of heart rate. Software QRS detection has been a research topic for decades and a common algorithmic structure is now shared by many algorithms. Before the actual detection, almost all algorithms use a filter to attenuate other signal components and artifacts. The most common filter is a bandpass filter with cut-off frequencies set at approximately 10 Hz and 25 Hz. After the filtering stage, a feature signal is generated in which the occurrence of a QRS complex is detected by comparing the feature against fixed or adaptive thresholds.

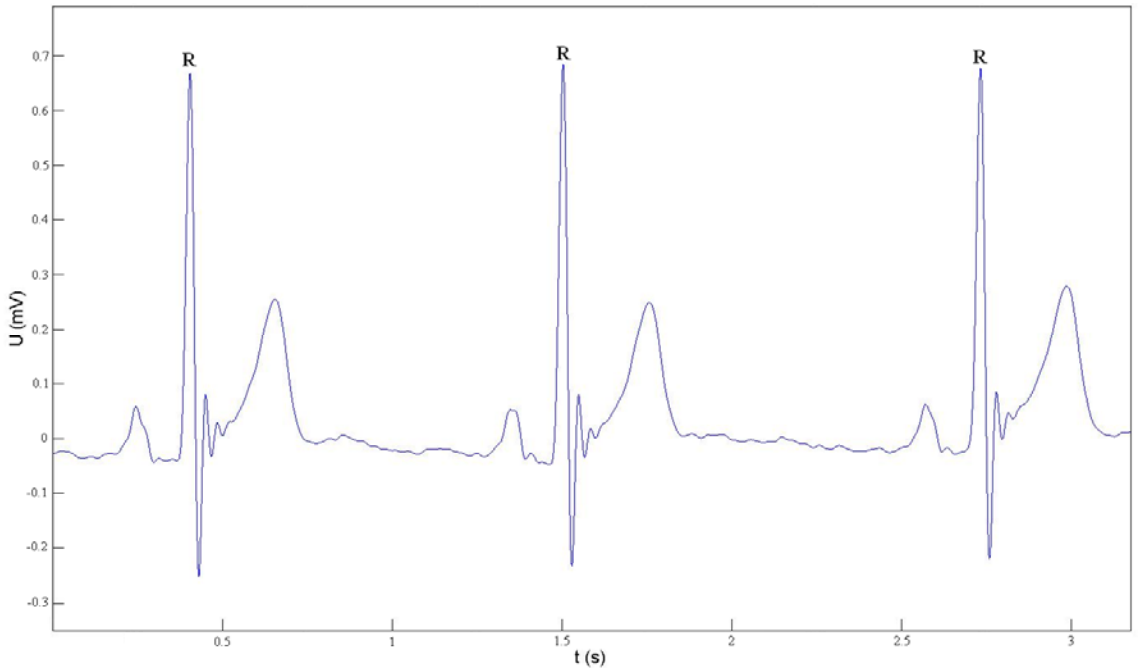

Figure 26: A typical ECG signal with the R-waves marked

For analysis of an ECG signal obtained from a stationary subject, it is often sufficient to use an amplitude threshold on the filtered signal, as the R-wave is significantly higher than all other components of the ECG waveform and clearly visible even in the presence of minor noise. However, more advanced algorithms are recommended for analysis of noisy signals. Some advanced algorithms include:

- Derivative-based algorithms. The characteristic steep slope of the QRS complex can be used for its detection. Typical feature signals are the first derivative, the second derivative or a linear combination of the two.
- Algorithms based on digital filters.
- Wavelet-based algorithms.
- Neural networks.

A detailed overview of advanced QRS detection algorithms is available in [Köhler, 2002].

QRS detection can be performed in real time with only a small delay. After electrodes are attached to the subject, a short training phase is usually necessary to correctly set the feature thresholds. Assuming a relatively noise-free environment where use of a complicated QRS detection algorithm is not necessary, the feature signal can be calculated practically in real time, as most basic QRS detection algorithms do not require anything more than a second derivative of the ECG signal. The delay caused by comparing the feature signal to thresholds is also negligible, allowing R-waves to be detected online with a barely noticeable delay in a relatively noise-free environment.

Once the R-waves have been located, RR intervals (heart periods) can be calculated as the time between two adjacent R-waves. During offline analysis, the R-waves are checked prior to calculation of RR intervals and abnormal R-waves (for instance, ectopic beats) are removed, leaving only normal healthy R-waves. The interval

between two normal R-waves is called the NN interval. Heart rate can be calculated directly from the NN intervals. During online analysis, we usually do not have the luxury of being able to remove abnormal R-waves, so RR intervals are used instead of NN intervals.

In a particular situation, the mean heart rate, the shortest interbeat interval, the longest interbeat interval, and the difference between the two are all of potential psychophysiological significance. During offline analysis, they can be calculated on any interval desired. During online analysis, the times of the last few R-waves are generally kept in memory and the significant variables are recalculated whenever a new R-wave is detected. The length of the buffer containing times of past R-waves depends on the situation. The minimal length of the buffer is limited by respiration; as heart rate varies with respiration, mean heart rate must be calculated over a time long enough to average out the changes in a single breath. The buffer size is limited upwards by the delays a large buffer causes: whenever a change in psychophysiological state affects heart rate, the new heart rate information must fill a majority of the buffer before it is noticed in the mean heart rate. A two-minute buffer, for instance, would completely neutralize respiration-related changes, but a significant change in heart rate would not be noticed in mean heart rate for at least half a minute. Since adult respiration rate is at least 10 breaths per minute, a tentative initial setting for buffer length would be fifteen seconds. This would allow mean heart rate to be averaged over several breaths, yet avoid introducing a too-long delay in the psychophysiological feedback loop. If fifteen seconds proves to be too short or too long an interval, it will be modified in the course of the project.

Heart rate variability was originally used for diagnostic purposes, but has also become an important psychophysiological tool. It can be estimated either in the time domain or the frequency domain. The following features can be calculated in the time domain:

- SDNN: standard deviation of the NN intervals,
- RMSSD: square root of the mean squared differences of successive NN intervals,
- NN50: number of interval differences of successive NN intervals greater than 50 ms,
- pNN50: NN50 divided by the total number of NN intervals.

Most of these measurements are highly correlated. RMSSD is preferred over NN50 and pNN50 because it has better statistical properties, but there is no harm in calculating all of them. All of these should be estimated from intervals of the same length.

In the frequency domain, heart rate variability is calculated as the total low-frequency power (0.04 – 0.15 Hz) divided by the total high-frequency power (0.15 – 0.4 Hz, basically identical to RSA). Generally, the power spectral density obtained using Welch's method is used. Frequency-domain analysis requires heart rate to be presented as an instantaneous time series with a constant sampling frequency. Heart rate derived directly from the length of RR intervals does not provide this information, as a new sample arrives whenever a new R-wave occurs. Interpolation is necessary to obtain an instantaneous time series.

Like the mean heart rate, heart rate variability estimates can be calculated over any interval desired when performing offline analysis. During online analysis, it again makes sense to keep the times of the last few R-waves in memory and recalculate the HRV estimates whenever a new R-wave is detected. Fifteen seconds is again recommended as a tentative initial setting for buffer length when calculating time-domain estimates of HRV. Frequency-domain analysis is more difficult. Theoretically, at least a two-minute recording is required to accurately estimate the low- and high-frequency power components. In addition, the mechanisms modulating heart rate should not change during the recording; the subject should maintain a more or less constant psychophysiological state during the two minutes. This cannot be guaranteed during online analysis, where the point is precisely to detect changes in the subject's state as they happen. Because of this, frequency-domain estimates of HRV are not recommended for online analysis. If we wish to perform a frequency-domain estimate in real time anyway, a second buffer is necessary in order to keep the last two or three minutes of the signal in memory. The power spectral density of the signal inside the buffer is then calculated and the power of the LF and HF bands is extracted.

The Simulink block diagram for online calculation of heart rate and time-domain heart rate variability is shown on Figure 27.

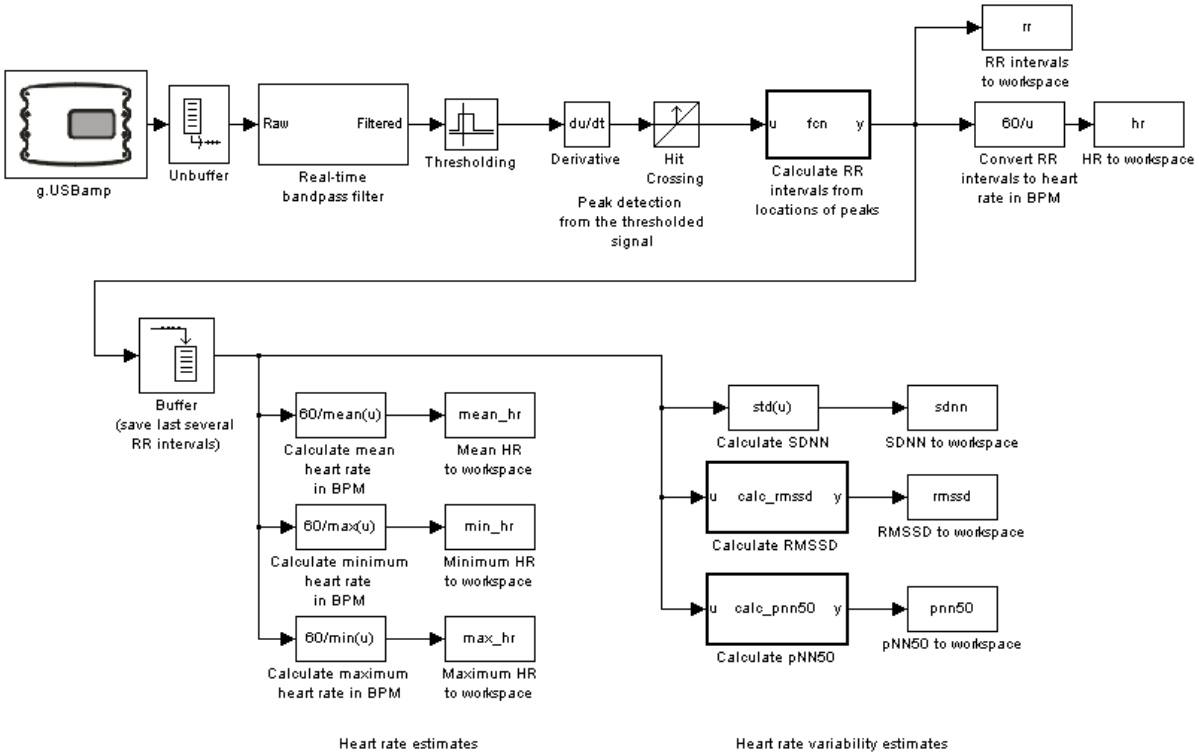

Figure 27: ECG analysis in Simulink

3.11.2 Electrodermal response

Electrodermal activity consists of two components: the skin conductance level and skin conductance responses. Skin conductance level is a measure of slow changes in electrodermal activity and can be obtained by simply averaging the signal over a certain period. Skin conductance responses (SCRs), on the other hand, are divided

into specific and nonspecific SCRs. Specific SCRs occur in response to a clearly defined stimulus. It is common to measure the time between the onset of the stimulus and the onset of the SCR, the amplitude of the SCR, the rise time and the half-recovery time. The algorithms used for this are fairly simple. Nonspecific SCRs occur in the absence of specific stimuli. For physiological purposes, the frequency and mean amplitude of nonspecific SCRs during a certain time period are calculated.

There are different ways to detect nonspecific SCRs. All of the partners currently use the algorithm provided by UPC. Two versions exist: one for offline analysis and one for real-time analysis. The algorithm for offline analysis first smoothes the original signal using a wavelet transform, then detects peaks based on derivative information. To avoid classifying upward baseline drifts as SCRs, a peak is discarded if the time between the beginning and end of the peak exceeds a certain threshold (5 seconds is recommended). To avoid classifying high-frequency information (such as noise) as SCRs, a peak is discarded if the difference between its maximum and minimum value is too low (0.05 or 0.1 μS is recommended for the minimum difference).

The algorithm for online analysis divides the signal into non-overlapping windows of a prespecified duration and then detects nonspecific SCRs separately inside each window. When recording begins, the algorithm records the electrodermal signal in a buffer until the buffer is full. Once it is full, the algorithm detects all SCRs in the windowed signal inside the buffer, then empties the buffer and begins recording anew. The windowed signal is not smoothed with a wavelet transform, as this could not be done in real time. Instead, the signal is convolved with a simple step filter that removes noisy frequencies. The cutoff level of the filter is determined using the signal's standard deviation, which provides a crude yet flexible measure of the noise present in the signal. Once the step filter is prepared, the Fourier transform of the windowed signal is multiplied by the filter and transformed back into the time domain. The problem with this filtering method is that the filtered signal is distorted at the edges due to missing samples at the beginning and end of the section. To alleviate this problem, it is possible to prefix and suffix the signal window with a small margin. The preceding few seconds of the signal are attached to the beginning of the window and the following few seconds are attached to the end of the window. This requires some minor changes to the filter in order to account for the larger size of the signal to be filtered. After the filtering, the margins need to be removed from the windowed signal. Once the windowed signal has been filtered, SCRs can be extracted from the window with the same peak detection method that was used in offline analysis.The optimal window width has not yet been determined, but it will mostly likely need to be at least thirty seconds to obtain a good estimate of SCR frequency.

The MATLAB code for offline and online detection of nonspecific SCRs is available.

3.11.3 Respiration

The respiration signal obtained from the SleepSense flow sensor is a relatively slow, clean signal (Figure 28). Smoothing with a lowpass filter is recommended, with a cutoff frequency set at approximately 0.5 Hz. Afterwards, a simple peak detection

algorithm (such as locating the minima and maxima of the signal) can be used to locate the peaks. The time between two peaks is called the respiration period and can be directly converted into respiration rate. The SleepSense flow sensor is not suitable for the calculation of any respiratory parameters other than respiration rate.

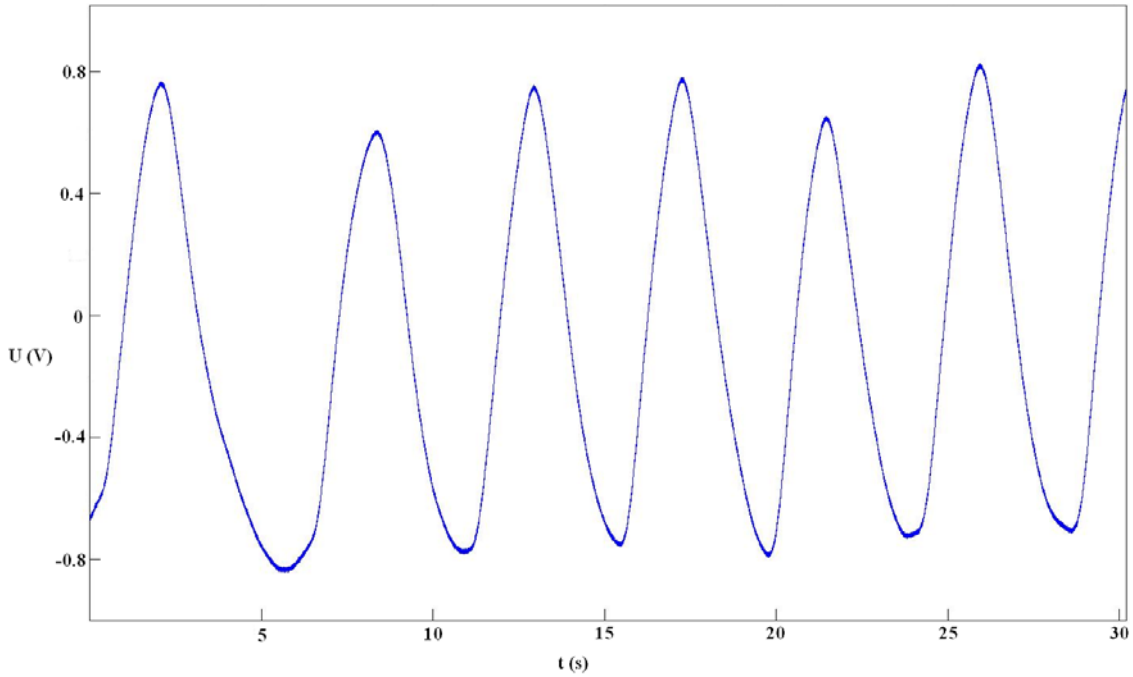

Figure 28: A sample signal from the respiration sensor

Online estimation of the respiration rate can be done with the same approach as during offline analysis: smoothing the signal and then using a simple peak detection algorithm. A slight delay is introduced by the peak detection algorithm, but this delay is brief. It is theoretically not necessary to average respiration rate, as any short-term changes are a direct result of the subject's psychophysiological state. However, if we do not mind a small delay, averaging respiration rate over the last few breaths may increase the accuracy of the estimation. This can be done by storing the last few respiration periods in a buffer, averaging them, and converting the mean respiration period into mean respiration rate. A tentative initial setting for buffer size would be three respiration periods. This would provide a reasonable average, yet avoid introducing large delays into a psychophysiological feedback loop. Of course, if the buffer size proves unsatisfactory, it can be changed during the course of the project.

The Simulink block diagram for calculation of respiration rate is shown on Figure 29.

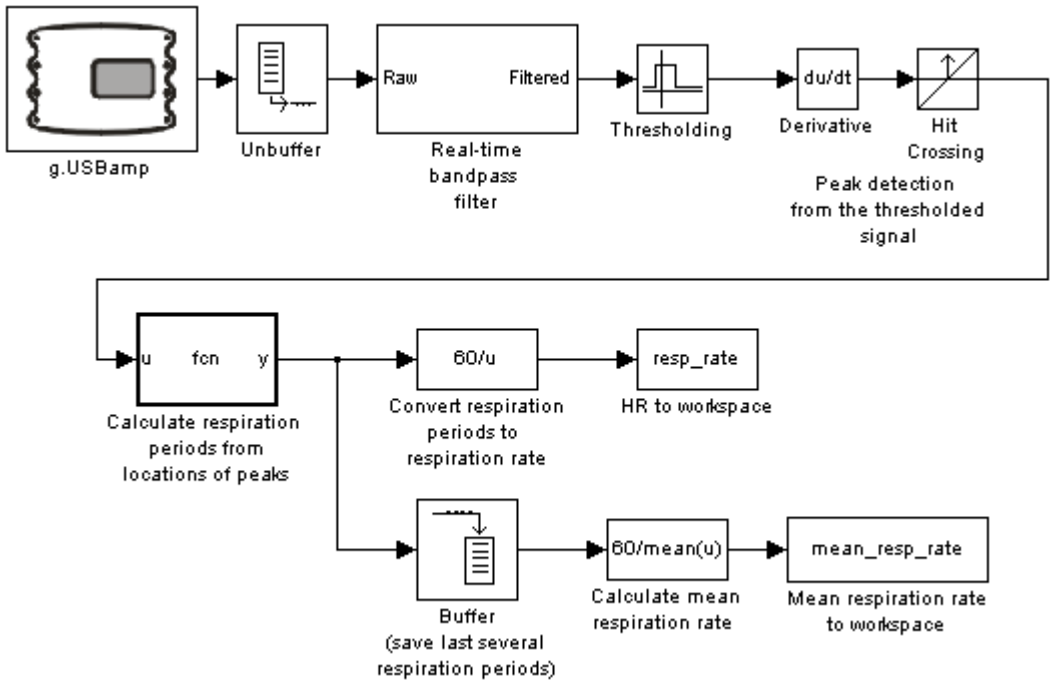

Figure 29: Calculation of respiration rate with Simulink

3.11.4 Blood pressure

The signal obtained from the continuous blood pressure sensor is a slow and clear signal while measured in a resting position but it is very sensitive to movement. A simple peak detection algorithm (minima and maxima) can be used to assess systolic and diastolic blood pressure.

3.11.5 Skin temperature

As a relatively slow signal, peripheral skin temperature is unsuitable for evaluation of psychophysiological responses to a single stimulus. It can, however, be effective when the subject maintains a constant emotional state for several minutes. In this case, it is possible to use either the mean temperature over the entire period or simply compare the value at the end of the time period to the value at the beginning. For online analysis, it is possible to simply use the current value of temperature or to average temperature over the last couple of seconds to remove the effects of measurement noise.

3.11.6 Pulse

The finger pulse signal ideally consists of clearly discernable peaks. Each heartbeat is characterized by a large peak followed by a smaller peak (Figure 30). Calculating heart rate from the finger pulse signal becomes a peak detection problem where care must be taken not to include the smaller peaks. For simple experiments where the subject is sitting down and the hand with the sensor is stationary, it is usually sufficient to filter the signal with a bandpass filter (with a bandpass of, for example, 0.1-30 Hz) and apply an amplitude threshold.

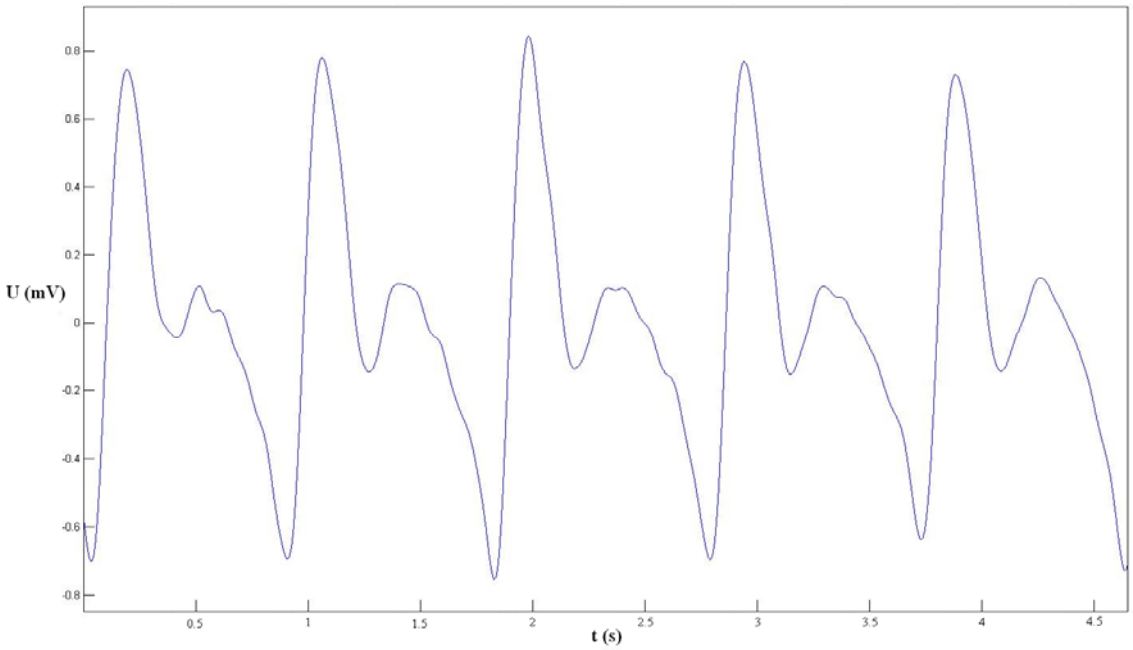

Figure 30: A sample signal from the finger pulse sensor

The moment when the heartbeat occurs is defined as the time when the signal reaches peak value (though other definitions, such as the time when the signal reaches 50% of the peak value, do exist). However, the finger pulse peak is much less 'sharp' than the R-wave in the ECG, so it is more difficult to calculate the exact heat rate. In addition, the finger pulse signal is much more vulnerable to movement artifacts than the ECG. Online analysis of heart rate can be done the same way as with the ECG signal.

3.11.7 Facial EMG

The raw EMG signal is subjected to a bandpass filter. Psychophysiologists have used different approaches to filtering the EMG. The traditional approach is to use a passband of approximately 30-400Hz, which should remove mechanical artifacts while preserving the electrical activity associated with muscle activation. However, some studies (Mandryk, 2006) have sampled the facial EMG with a very low sampling frequency (32 Hz) and therefore evaluated only the low-frequency component of the EMG. The frequency band beneath 16 Hz should consist mainly of mechanical artifacts. However, even in these cases useful data was obtained from the signal. Both approaches are worth looking into. Additionally, since the signal from the zygomaticus major is affected by speech, sections where the subject is speaking are not suitable for analysis.

Regardless of the cutoff frequencies, most psychophysiological studies rectify the filtered signal. The rectified signal can be averaged over a particular time period (either online or offline) or evaluated directly. If the signal is being averaged over a particular time period, another feature that may be worth looking into is the RMS value. However, to our knowledge no psychophysiological studies thus far have used the RMS value or done any spectral analysis of the EMG signal, an approach that may perhaps prove fruitful.

3.11.8 EEG

The continuous EEG, sampled with 500Hz is recorded (Acticap, Brain Products, Munich, Germany) using 30 scalp electrodes (Active Ag/AgCl electrodes) placed according to the international 10-20 system [Jasper, 1958]. Two additional electrodes are applied below the outer canthus of each eye. The ground electrode is placed at the AFz position (see black GND circle on Figure 31). An average reference over all electrodes serves as point of origin with zero potential. The impedance for all electrodes is kept below 20kΩ. The EEG measurements were done as part of a master thesis at the University of Zurich [Schumacher, 2008].

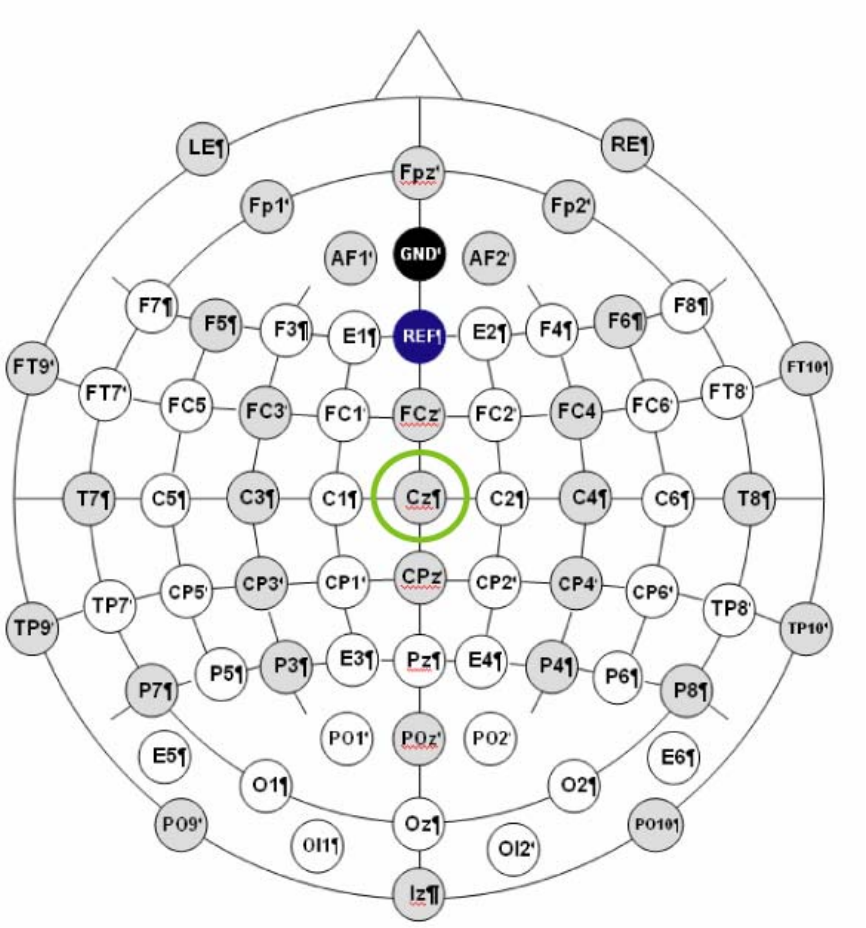

Figure 31: Positions of the 32 electrodes with ground

3.11.9 EMG of lower leg muscles

Leg muscle (TA, GM) activity from both legs are recorded through bipolar Ag/AgCl electrodes (inter-electrode distance 25mm). EMG recordings are amplified, filtered (bandpass 30-300 Hz) and sampled at 1000 Hz via a 12-bit A/D-converter. Trigger signals provided by the Lokomat that identify the onset of stance phase are additionally recorded. Signals are analysed using Soleasy (ALEA Solutions GmbH, Zurich). Locomotor EMG activity was analyzed using the RMS value per stride smoothed by a moving window average (window width: 25 strides, which is equivalent to about 1 min of walking).

3.12 Evaluation of the proposed methodology

3.12.1 Upper extremities

3.12.1.1 Tasks

Two different tasks have been prepared: a purely cognitive task and a hand-eye coordination task. Each subject performs the cognitive task by itself, the coordination task by itself, and both tasks at the same time. The order in which the tasks are performed is randomized.

The cognitive task presents the subject with two numbers that must be multiplied. These numbers are randomly generated between zero and thirty. Four possible answers are shown immediately underneath. Using a headset and the Dragon NaturallySpeaking 9.0 speech recognition software, the subject must verbally choose the answer they believe is correct (by saying “first”, “second”, “third” or “fourth” in Slovenian). If the subject answers correctly, their choice is coloured green. If the subject answers incorrectly, their choice is coloured red and the correct choice is coloured green. The subject has fifteen seconds to answer each question; if they fail to answer within that time, the result is identical to making an incorrect choice (except that no number turns red). The time remaining is displayed using a large bar next to the numbers which grows progressively shorter and turns from green through yellow to red as time runs out. After a choice is made or the time runs out, there is a five-second pause, and then the next two numbers to be multiplied are generated. A screenshot of the display is shown on Figure 32.

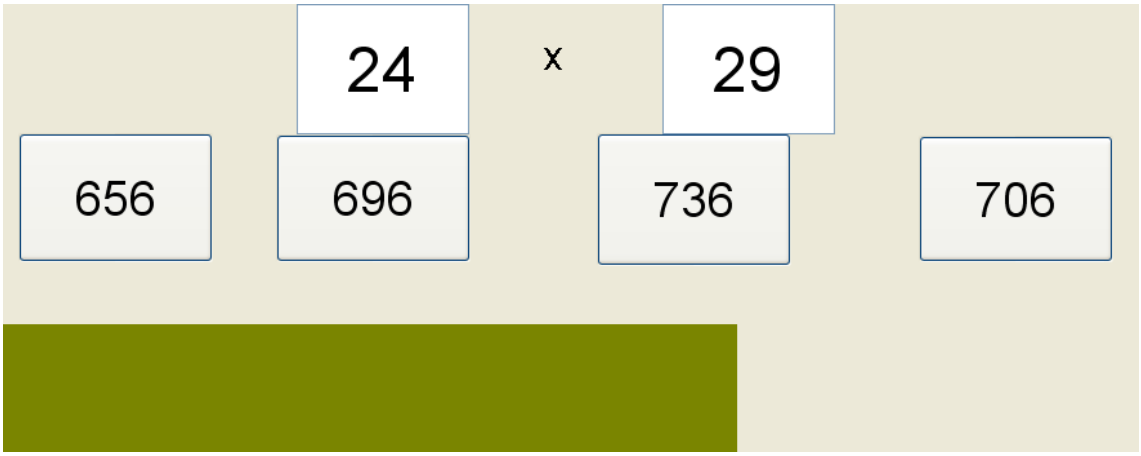

Figure 32: Computer display for the cognitive task

The hand-eye coordination tasks presents the subject with the classic inverted pendulum control problem. A thin pole with a weight at its top end is attached at its bottom to a moving cart. This vertical pendulum is inherently unstable and must be actively balanced by moving the cart horizontally. The subject receives a presentation of a simulated cart and pole on the computer screen and moves the cart using a Phantom system. Moving the end of the Phantom to the left moves the cart to the left and moving the end of the Phantom to the right moves the cart to the right. Haptic feedback that simulates the resistance of the cart is provided to the subject. The model dynamics are adjusted in such a way to make balancing the pendulum

moderately challenging. If the subject fails to balance the pendulum and it falls to a horizontal position, it is immediately reset to a nearly vertical position. A screenshot of the display is shown on Figure 33.

Before performing the hand-eye coordination task, the subject spends a few minutes moving the Phantom in any way he or she desires with the computer screen turned off. This part of the experiment is meant to evaluate the effect physical effort by itself (with no mental effort) has on the pyschophysiological signals.

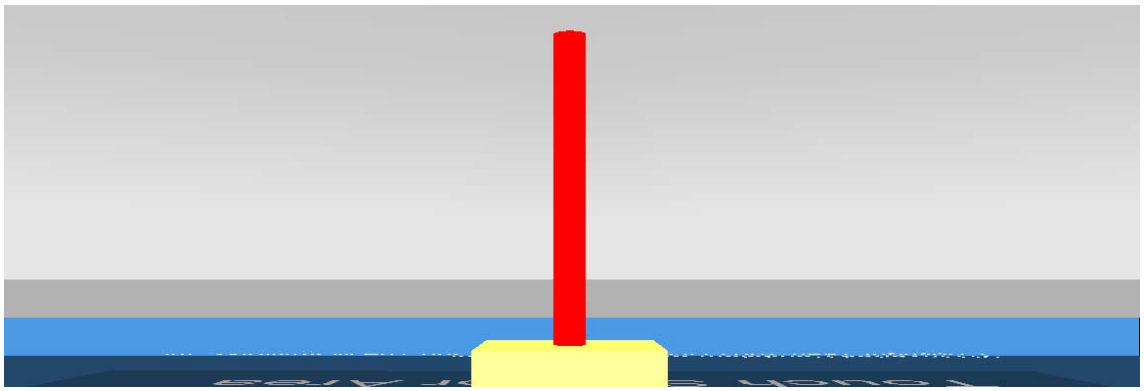

Figure 33: Computer display for the hand-eye coordination task

When the subject must perform both tasks simultaneously, the displays are both shown on the same monitor, one above the other. Preliminary tests have shown that the cognitive task does not draw the subject's gaze from the coordination task very much. For the cognitive task, the subject only needs to focus on the display in order to read the two numbers and then to check which of the four options is correct. A screenshot of the display is shown on Figure 34.

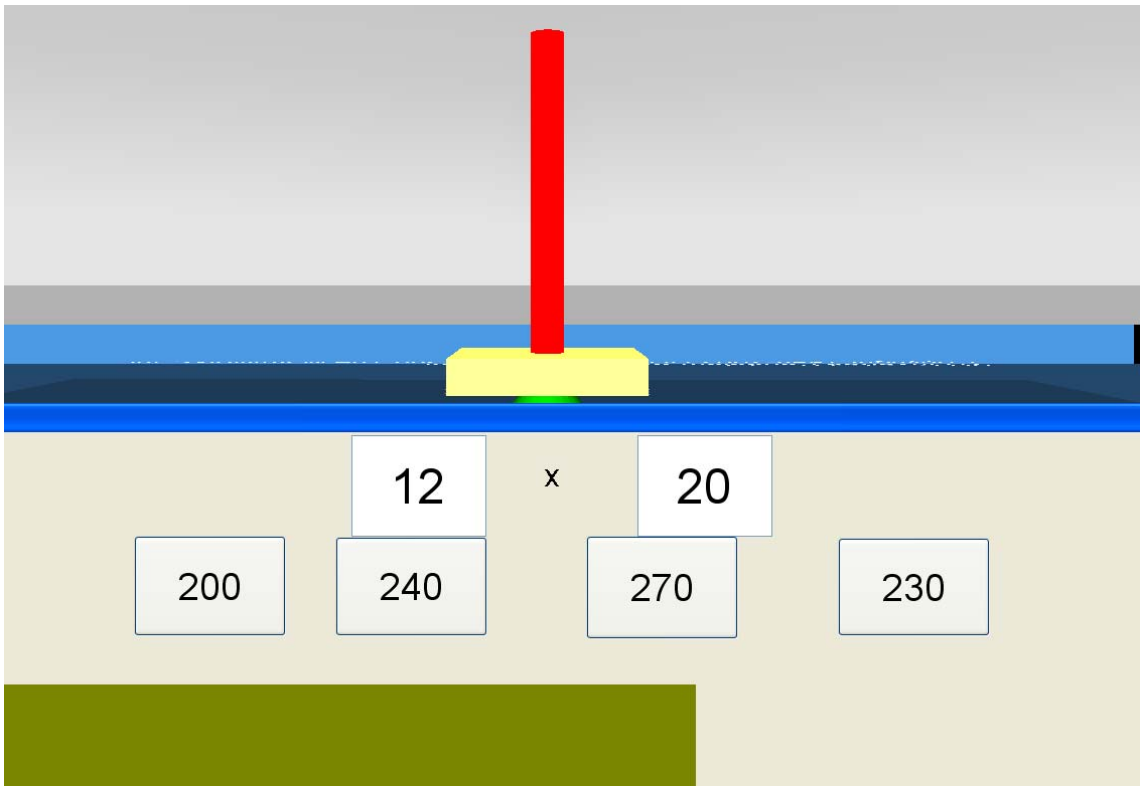

Figure 34: Computer display for both tasks at once

A photograph of a subject performing the hand-eye coordination task is shown in Figure 35.

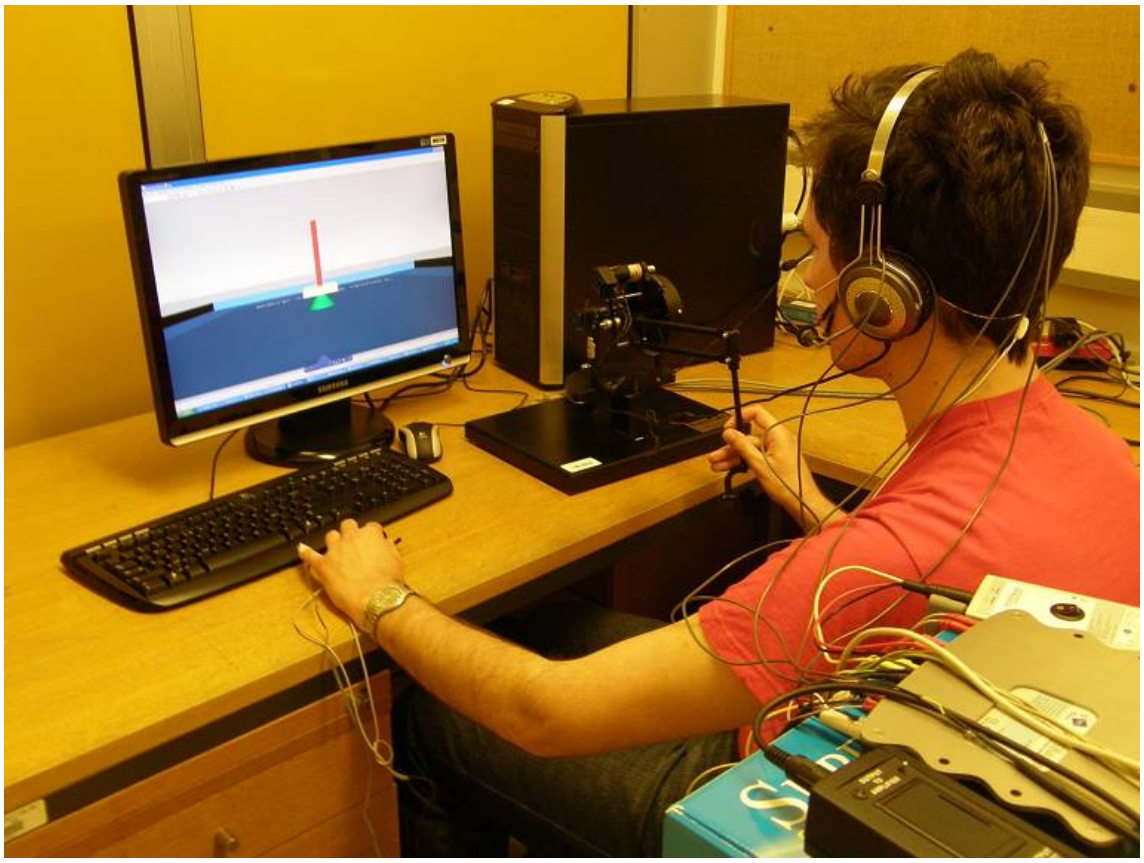

Figure 35: Subject performing hand-eye coordination task

3.12.1.2 Procedure of the experiment

The experiment proceeds as follows:

- the subject signs the informed consent form
- the subject arrives in the lab (the experiment is conducted in a quiet area where external stimuli do not disturb the subject)
- the measurement equipment is attached and turned on
- the experiment procedure is explained to the subject and the two tasks are presented
- the subject spends a few minutes practicing both tasks
- signals are monitored until the subject becomes used to the environment (ie. most effects of nervousness or novelty pass)
- the subject rests for five minutes so that baseline measurements can be obtained
- the first task (randomly chosen) is performed for five minutes
- a few self-evaluation questions are asked, and then the subject rests for five minutes
- the second task (randomly chosen) is performed for five minutes
- a few self-evaluation questions are asked, and then the subject rests for five minutes
- the third task (randomly chosen) is performed for five minutes

- a few self-evaluation questions are asked, and then the subject rests for five minutes
- the subject is given a few final questions about their experience

3.12.1.3 Questionnaire

The questions that the subject is asked during the breaks have been suggested by psychologists from the Faculty of Arts and are as follows (translated from Slovenian):

For the last task, please mark the average intensity of the following emotions:

	0 – did not feel	1 – very mild	2 – mild	3 – moderate	4 – strong	5 – very strong
Happiness						
Frustration						
Concentration						

For the emotions that you did feel, please sketch how their intensity changed during the task.

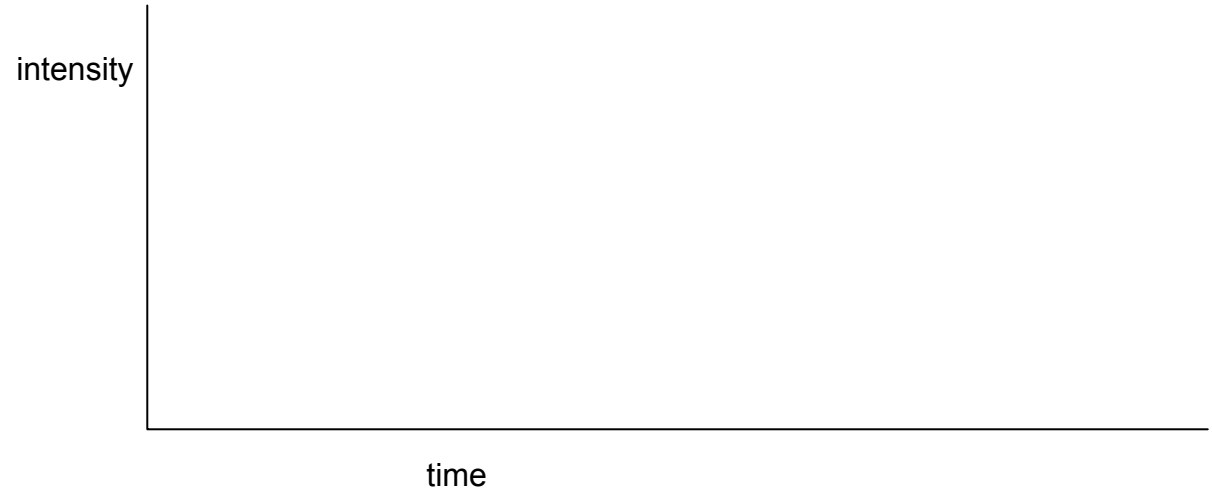

On a scale from 1 to 5, estimate how hard you found the task to be (1 – very simple, 5 – very difficult).

1 2 3 4 5

When performing two tasks at once, how much was your performance affected due to divided attention (1 – not affected at all, 5 – very strongly affected / impossible to perform both tasks at once)?

1 2 3 4 5

Estimate your level of concentration and emotional state on the graph below by marking the place where you are ‚located'. The horizontal position is your emotional state. -5 represents very negative feelings, 0 represents a neutral state and 5 represents very positive feelings. The vertical position is your concentration level. 0 means that you did not focus on the task at all while 5 means that you were completely focused on the task.

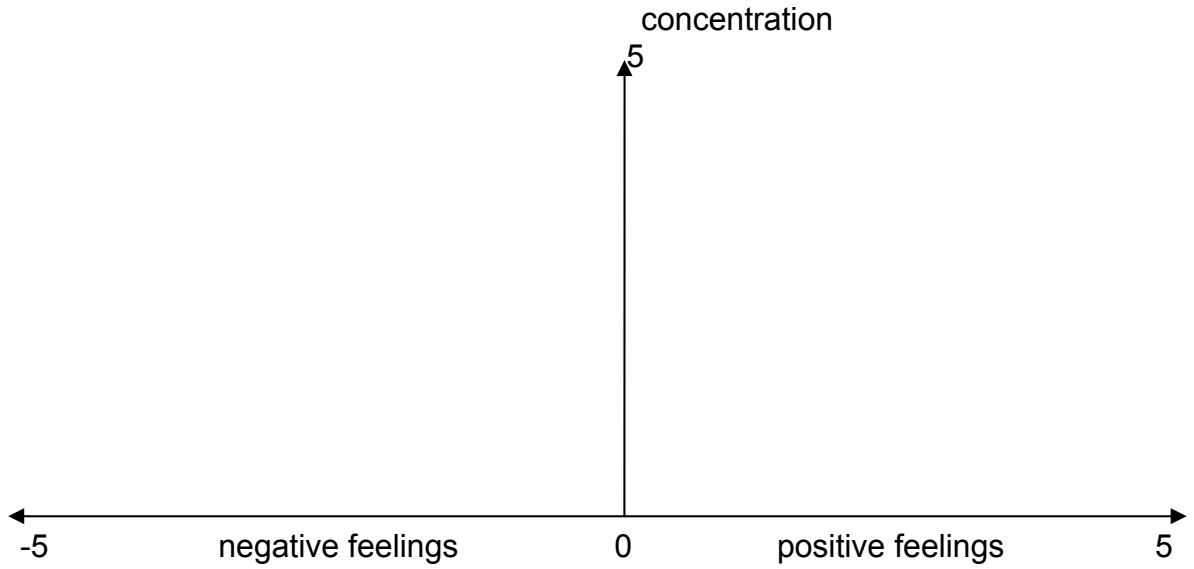

3.12.1.4 Subjects

Twelve subjects participated in the experiment. All were healthy males between the age of 22 and 41 (mean age 27.7, median age 27, standard deviation 5.6 years). All were either students or researchers from the Faculty of Electrical Engineering in Ljubljana. None had consumed coffee or alcohol or smoked cigarettes on the day of the experiment.

3.12.2 Lower extremities

In order to evaluate all potential psychophysiological measured variables, ETH conducted three different experiments. In experiment 1, the feasibility of EEG measurements in the Lokomat was assessed. In experiment 2, heart rate, heart rate variability, electrodermal activity, skin temperature and respiration rate were tested. Experiment 3 tested the feasibility of continuous blood pressure measurement, EMG and ergospirometry.

3.12.2.1 Experiment 1 (Feasibility of EEG Measurements)

A simple measurement setup was used to assess whether or not EEG measurements can be recorded reliably during Lokomat walking in VR. Subjects had to walk in the DGO without any additional task to fulfil. EEG was measured over 10 minutes. A body weight support of 70% was used. In order to test the feasibility of the chosen approach, the EEG was visually checked for artifacts. Secondly, a topographical cluster algorithm was applied triggered to the left heel strike in order to determine if different cortical processes can be linked to different phases of the gait cycle. These comparisons were used to judge the feasibility of the chosen approach.

Figure 36: Subject walking in the Lokomat wearing EEG sensors

3.12.2.2 Experiment 2

We investigated ECG, electrodermal activity, joint torques, respiration rate and skin temperature during seven different conditions. We discriminated between physical tasks, cognitive tasks and both tasks at the same time. The order of the tasks was randomized.

T1: Baseline: Subjects stood still in the Lokomat.
T2: Walking I: Subjects walked in the Lokomat with 25-30 % body weight support. No VR scenario was presented while walking.
T3: Walking II: Subjects walked in the Lokomat and a VR scenario (walking through a city) was presented (cf. Figure 37a).
T4: Walking III: Subjects walked in the Lokomat and had to play virtual football against an opponent in a VR scenario. If subjects performed well they walked faster than the opponent (cf. Figure 37b).
T5: Walking IV: Subjects walked in the Lokomat and in a VR scenario where they had to cross a canyon on a narrow bridge (cf. Figure 37c).
T6: Cognition I: Subjects had to repeatedly subtract 7 from a four-digit number while standing still in the Lokomat.
T7: Cognition II: Subjects had to perform T6 while walking in the Lokomat.

a. T3 Walking with VR

b. T4 Walking with VR and physical task

c. T5 Walking over canyon

Figure 37: Screenshots of VR scenarios during different tasks

3.12.2.3 Experiment 3

In experiment 3, we measured continuous blood pressure, EMG and ergospirometry in the same setting as used in experiment 2.

3.12.2.4 Procedure of experiment 1

The experiment proceeded as follows:

- the subject signs the informed consent form
- the subject arrives in the lab (the experiment was conducted in a quiet area where external stimuli did not disturb the subject)
- the experiment procedure is explained to the subject
- the measurement equipment (EEG) is attached to the subject.
- the Lokomat is attached to the subject and the subjects walk in the Lokomat to get familiar with the device.
- the measurement equipment (EEG) is attached to the subject.
- EEG measurements are performed while subjects walk in the Lokomat.

3.12.2.5 Procedure of experiment 2

The experiment proceeds as follows:

- the subject arrives in the lab (the experiment is conducted in a quiet area where external stimuli do not disturb the subject)
- the measurement equipment is attached and turned on
- the experiment procedure is explained to the subject
- tasks one through seven are presented to the subject. The order of occurance was randomized to exclude changes in e.g. heart rate or electrodermal activity due to fatigue.
- each task is performed three minutes.

3.12.2.6 Procedure of experiment 3

The procedure is the same as in experiment 2.

3.13 Preliminary results of the evaluation studies

3.13.1 Upper extremities

Results of the preliminary study revealed notable differences between baseline and tasks as well as between the three tasks. First of all, results of the self-evaluation questionnaires showed marked differences between the tasks. These differences are presented in Table 2.

Table 2: Results of self-evaluation questionnaires

	coordination task	cognitive task	both tasks at once
mean satisfaction	2,42	2,67	1,75
mean frustration	1,33	1,33	2,58
mean concentration	3,25	3,83	4,42
mean difficulty	2,82	3,25	4,25

Subjects found the hand-eye coordination task to be easiest and to require the least concentration, while performing both tasks at once was hardest and required the most concentration. Satisfaction was highest during the cognitive task and lowest when performing both tasks at once. Frustration was about equal for the coordination task and the cognitive task, but increased when performing both tasks at once.

The strongest task effect was detected in electrodermal activity, specifically the frequency of nonspecific skin conductance responses. The subjects can be divided into two groups: those with a low baseline frequency of nonspecific SCRs and those with a high baseline frequency of nonspecific SCRs. Because of this, the frequency of SCRs during each task period was evaluated as the percentage increase from baseline. A graph of the results is shown on Figure 38. For our subjects, the frequency of nonspecific SCRs did not, in general, increase from baseline to motor movement: there was actually a mean decrease of 9% from baseline while subjects randomly moved the Phantom. The frequency of nonspecific SCRs did, however, increase by an average of 87% from baseline to the hand-eye coordination task, so the mental effort was clearly the principal influence. The increase in nonspecific SCR frequency was even more pronounced during the cognitive task (mean increase of 119% from baseline) and when performing both tasks at once (mean increase of 170% from baseline). These findings agree with previous studies which have shown that electrodermal activity represents a measure of arousal, as the frequency of SCRs correlates with self-reported concentration.

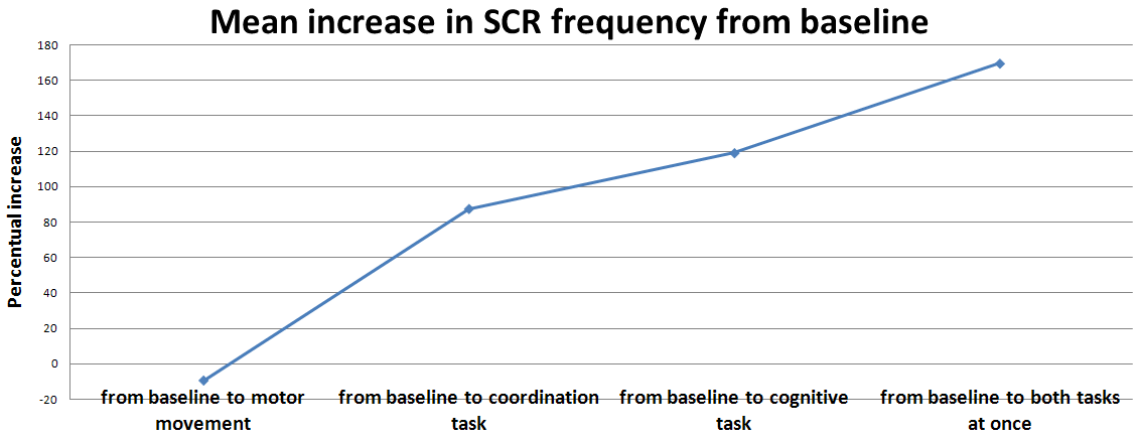

Figure 38: Increase in frequency of nonspecific SCRs from baseline to task

Though the task effect was not as marked as in nonspecific SCR frequency, tonic skin conductance level was different between baseline and task in most subjects (Figure 39). During rest, tonic SCL tended to decrease in almost all subjects, a finding at odds with some studies that did show tonic SCL drifting upward with time. Tonic SCL did increase during tasks, and appeared to be unaffected by motor movement. It increased by an average of 0.005 μS from baseline to motor movement, 0.6 μS from baseline to the hand-eye coordination task, 1.2 μS from baseline to the cognitive task and 0.7 μS from baseline to both tasks. Tonic SCL is apparently not a measure of concentration, but some other aspect of psychophysiological state.

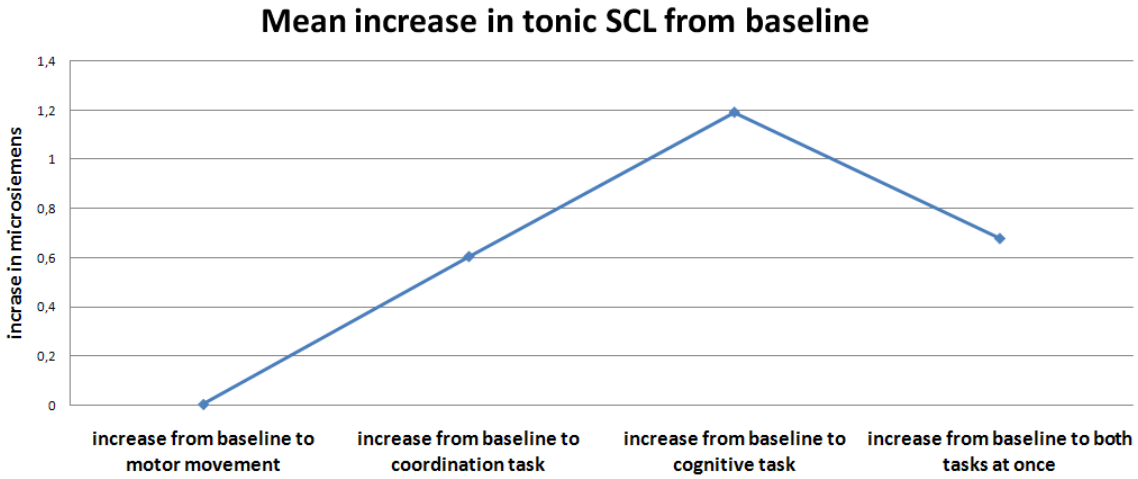

Figure 39: Increase in tonic SCL from baseline to task

Heart rate did not show a consistent change from baseline to task. Although a number of subjects exhibited a reliable increase in heart rate from baseline to task, there were also a number of subjects whose heart rate did not seem to be at all affected. On average, heart rate increased by a mere 0.1 beats per minute from baseline to motor movement without mental effort. It decreased from baseline to the hand-eye coordination task by 0.2 beats per minute. It did, however, increase by an average of 1.8 beats per minute from baseline to the cognitive task and 2.5 beats per minute from baseline to both tasks at once (Figure 40). Heart rate increases have been linked to stress, and this may be a good explanation for our results. Those

subjects who did not find the experiment to be at all stressful did not exhibit an increase in heart rate. However, those subjects who found the experiment stressful exhibited larger increases in heart rate during more stressful situations. The cognitive task can be considered more stressful than the hand-eye coordination task as it presents more difficult questions and is timed to ensure more pressure on the subject. Performing both tasks is naturally the most stressful of all. However, the stress explanation may be false, and further experiments will be necessary to establish a clear relationship between heart rate and psychological state.

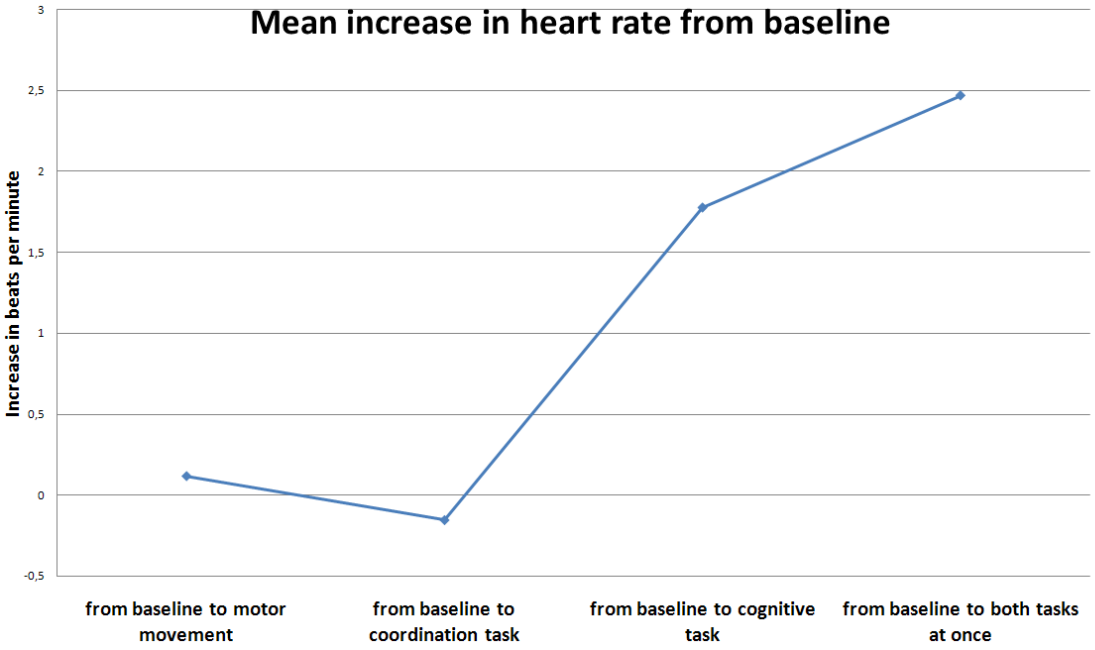

Figure 40: Increase in heart rate from baseline to task

Most of the measures of heart rate variability also appeared somehow connected to arousal/concentration, with the highest increases measured when performing both tasks at once and the lowest increases measured during motor movement. However, there were many outliers. Additionally, for some of the subjects HRV increases and decreases were exactly opposite to the general trend, increasing when they would be expected to decrease and vice-versa. Though the preliminary experiment has shown a connection between HRV and psychological state, more experiments will be needed to establish the nature of this connection.

Calculating heart rate from finger pulse gives results very similar to those obtained from the electromyogram. However, since the finger pulse is extremely susceptible to movement, it is not recommended for future research. Variables such as pulse transfer time (the time between a peak in the ECG and its corresponding peak in the finger pulse) are virtually impossible to accurately calculate.

Peripheral skin temperature, though a slow indicator, regularly decreased from baseline to task and then increased once again during the following baseline. Skin temperature increased by an average of 0.35 ^{O}C from baseline to motor movement. It decreased by an average of -0.3 ^{O}C from baseline to the hand-eye coordination task, -0.62 ^{O}C from baseline to the cognitive task and -1.08 ^{O}C from baseline to both tasks at once (Figure 41). Skin temperature appears to be linked to concentration.

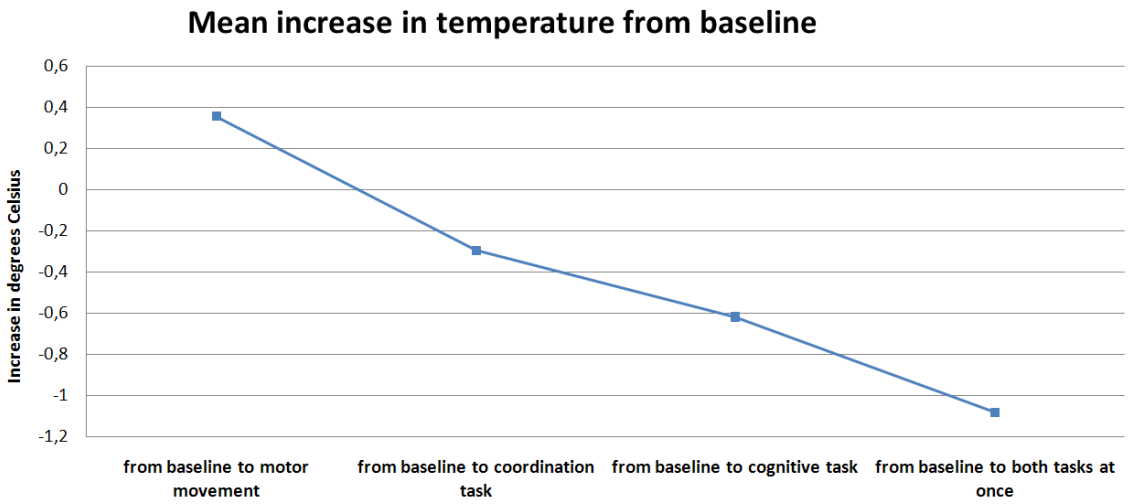

Figure 41: Increase in peripheral skin temperature from baseline to task

Respiration rate increased from baseline to task in nearly all subjects. Respiration rate increases from baseline to task even in subjects who do not show any change in heart rate. The disadvantage of the use of respiration rate for analysis is that it is extremely susceptible to the effects motor movement. In our experiment, respiration rate increased (on average) by 18.8% from baseline to motor movement, 21.2% from baseline to the hand-eye coordination task, 24.0% from baseline to the cognitive task and 18.4% from baseline to both tasks at once (Figure 42). It is currently unclear why the average increase in respiration rate was lowest from baseline to both tasks at once.

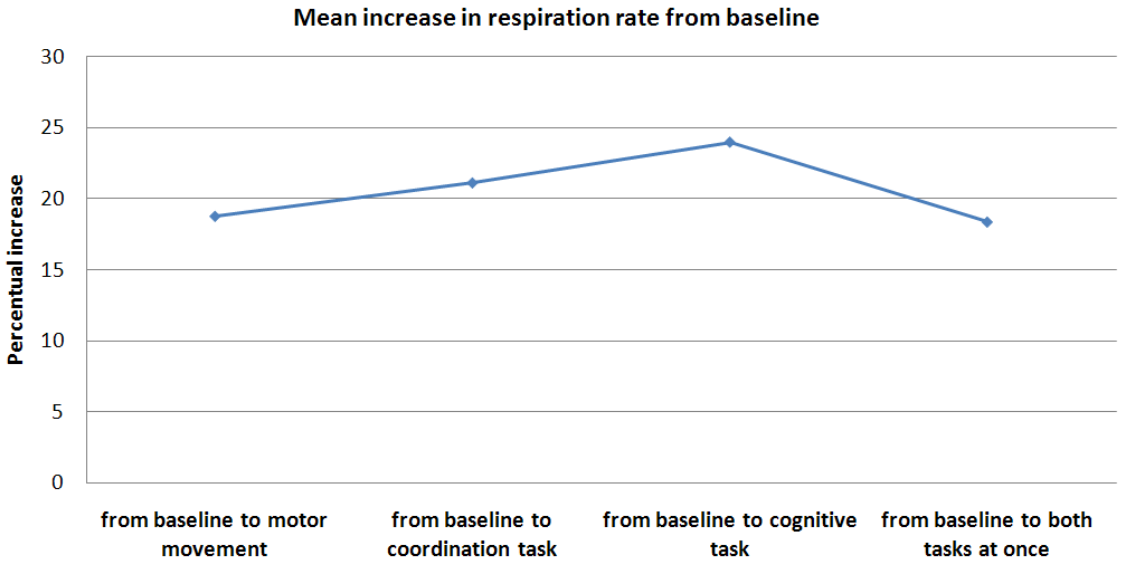

Figure 42: Increase in respiration rate from baseline to task

Though responses to several events (such as a particularly difficult question) were visible in the facial EMG signal, the electrodes were too prone to movement artifacts to obtain a good signal. Therefore, any results are unreliable. If facial EMG is used in the future, better electrodes and cables will be needed to minimize artifacts.

Though we have not yet established a clear relationship between different psychophysiological signals and psychological states, it is clear that we can successfully record and analyze the signals. Moreover, it has been confirmed that relationships do exist between the signals and psychological states. This experiment, along with the one performed by ETH, provides a basic groundwork for further psychophysiological studies within MIMICS.

3.13.2 Lower extremities

3.13.2.1 Experiment 1 (Feasibility of EEG Measurements)

Movement artifacts: Cable dragging
Although the cables were actively shielded, head movement caused cable dragging in some subjects (see Figure 43). Obvious artifacts were removed using independent component analysis (ICA) or not included in the analysis if the amplitude exceeded ±80µV

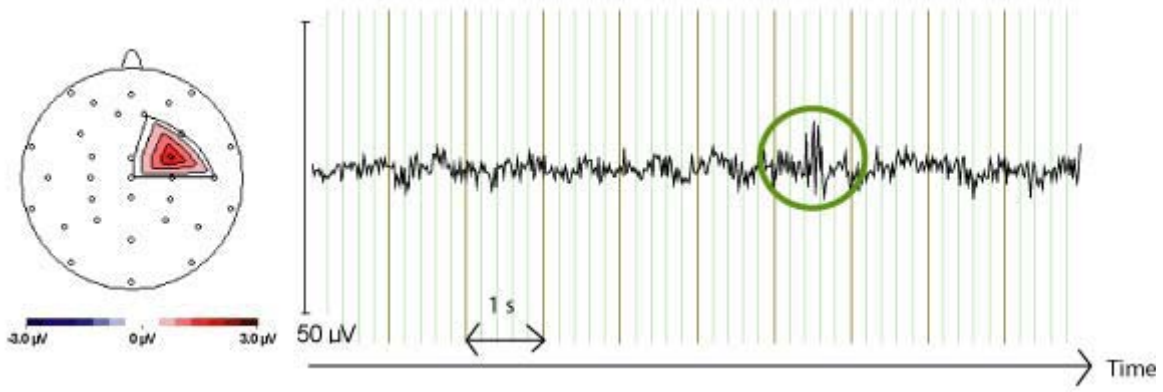

Figure 43: Cable dragging on FC4-channel (see green circle) in one subject, visible as an independent component in ICA.

Eye movement artifacts
Eye movement artifacts were a major problem in EEG measurements in the Lokomat in combination with virtual reality. Some artifacts remained even if subjects were asked to close their eyes. Eye movements that were not linked to the gait cycle could successfully be reduced offline using ICA. However, not all of the eye movement artifacts could be removed since this movement was temporally closely related to the cortical activity of interest. Removing all eye movement artifacts would have resulted in the removal of the activity of interest (Figure 44).

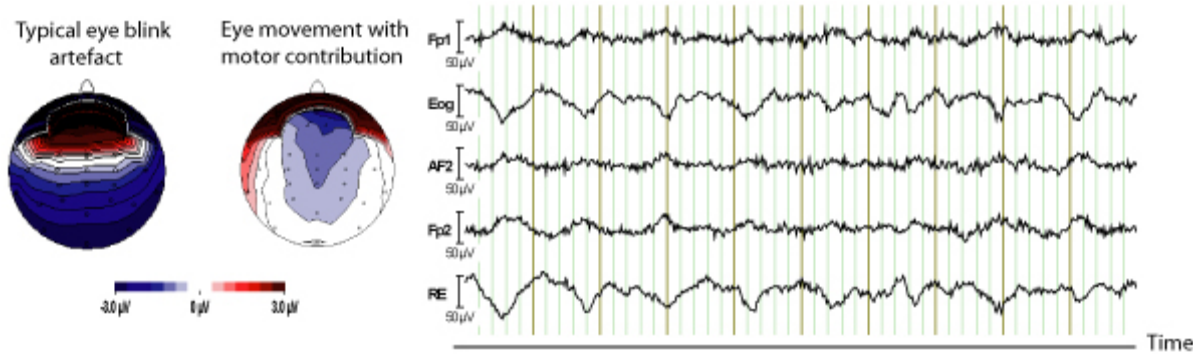

Figure 44: Eye movement artifacts in filtered EEG data of one subject (right side). Eye movement artifacts on Eog (left eye) and RE (right eye) channel were characterized through slow oscillations and eye movement coupled on central activity in one subject, visible as an independent component in ICA (left side). Another independent component (representing isolated eye blink) is shown for comparison.

Our results showed that EEG is not yet an appropriate method to detect brain activity during walking in virtual reality. While walking in VR, subjects have to move their eyes to capture the whole scenario. These eye movements result in artifacts that can not be completely removed without also removing significant information from the signal. EEG measurements will not be used in further psychophysiological measurements.

3.13.2.2 Experiment 2

Similar to the upper extremity experiments the psychophysiological signal with the highest task-sensitivity was the electrodermal activity. Nonspecific skin conductance responses seem to be a measure of arousal. The pure motor movement (Task2 & Task3) did not significantly increase SCRs compared to baseline (Task1)
Motor movement combined with a cognitive task (Task7), with a motor task (Task4; football playing) or with a psychologically challenging task (Task5; walking over a canyon) significantly increased SCRs compared to baseline task. Also, the cognitive task (Task6) increased SCRs significant. Results are shown in Table 3.
Therefore we suggest that SCRs reflect arousal. This goes in line with previous studies showing that electrodermal activity represents a measure of arousal.

Table 3: Frequency of nonspecific SCRs during all tasks.

Task	**T1**	**T2**	**T3**	**T4**	**T5**	**T6**	**T7**
SCRs	2	8	10	20	24	25	25
stdev	1.3	7.0	14.7	13.4	10.9	7.5	10.8

Results of our heart rate (HR) recordings showed that motor movement in the Lokomat resulted in an increase in the HR in every subject. This demonstrates that

HR is strongly affected by physical load (results are shown in Table 4). Nevertheless HR also increased in the cognitive task without motor movement. Subjects reported that the cognitive task was very challenging and induced stress to them. Our results suggest that HR not only reflects physical load but can also reflect stress. Further experiments are necessary to confirm this observation.

Table 4: Results for mean heart rate, standard deviation of heart rate and pNN50

Task	T1	T2	T3	T4	T5	T6	T7
mean HR (beats/min)	74	89	85	109	92	100	91
Stdev	12.1	17.4	9.5	17.6	22.4	24.4	19.4
pNN50	0.32	0.29	0.28	0.01	0.18	0.10	0.17

Our results for heart rate variability (HRV) were not consistent. There seems to be a relationship between the course of HRV and SCRs indicating a connection to arousal/ concentration. But there was a large variability between the subjects. Further experiments have to be done to establish the relevance of HRV.

Results from peripheral skin temperature do not show a strong link to mental concentration. In all tasks (except the baseline task) temperature decreased in the first minute but then increased again due to the movement induced by the Lokomat.

Breathing frequency (BF) increased in all tasks compared to baseline. We could not assess BF in the cognitive tasks (T6 & T7), as these tasks demanded speaking. The respiration sensor is not capable of measuring BF as soon as the subject wearing the sensor is speaking. Therefore additional measurements methods have to be assessed to record BF even when subjects are talking. Table 5 shows the results for BF during tasks T1-T5.

Table 5: Results for breathing frequency

	T1	T2	T3	T4	T5	T6	T7
BF (breaths/min)	12	20	21	26	25	-	-
stdev	3.9	3.8	3.9	6.0	6.6	-	-

Our results from the Biofeedback calculations from the Lokomat showed that all subjects had significantly increased biofeedback values from baseline to the challenging task 4 (football playing). The biofeedback can be used to detect voluntary and involuntary muscle activity (Table 6).

Table 6: Results for biofeedback values. All values were normalized to T2.

	T1	T2	T3	T4	T5	T6	T7
BF Hip	-	0	+1.6	+26.9	+3.1	-	+0.5
BF Knee	-	0	+0.6	+16.7	+0.3	-	+1.0

3.13.2.3 Experiment 3

Continuous blood pressure measurements show that this recording method is highly sensitive to movement. As we were not able to completely eliminate the movement artefacts, we were not able to obtain a useful signal. Additionally the device for measuring continuous blood pressure evoked strong artefacts on all the other signals. Therefore we will exclude these measurements from further experiments.

Results of EMG measurements of lower extremities showed that higher TA and GM activity can be measured during soccer playing in Task 4 than in the other tasks. RMS values of the different conditions did not significant differ from each other. Results are shown in Figure 45.

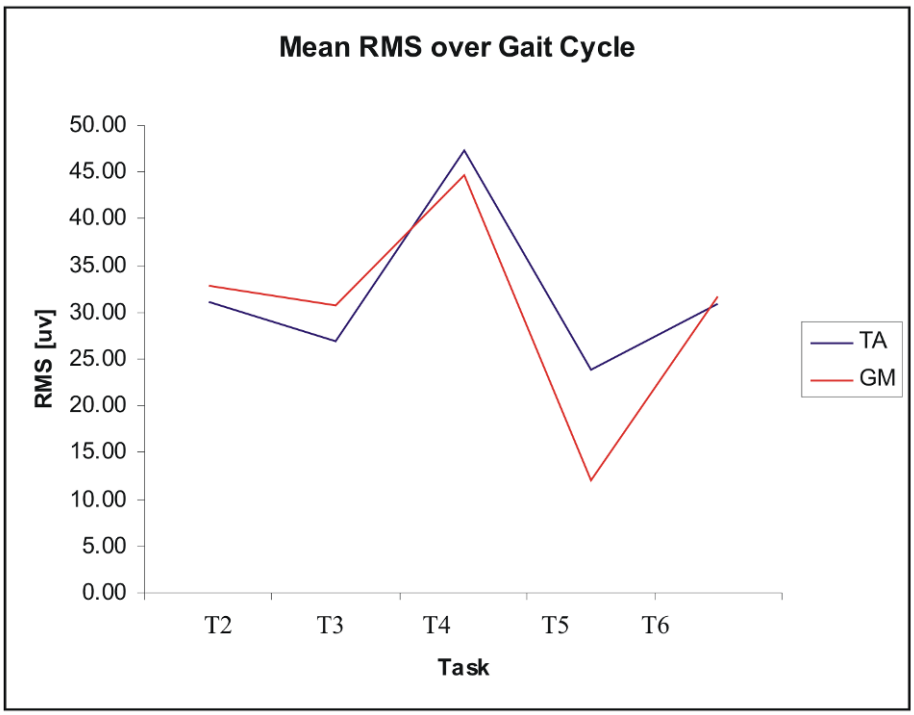

Figure 45: Locomotor EMG activity was analysed using the RMS value per stride

The facial electromyography signal was not applicable to detect eye blinking. The signal was too sensitive to eye movements and we were not able to differentiate between eye blinking and eye movement. If eye blinking has to be detected, another approach has to be developed.
In ergospirometry measurements we analyzed minute ventilation (VE), tidal volume (VT), respiratory frequency (RF), respiratory quotient (R), O_2 consumption (VO_2) and CO_2 production (VCO_2). All parameters were also assessed during cognitive tasks. Task 5 (walking over a canyon) was not assessed. Although all parameters changed significant ($p<0.05$) over all tasks we were not able to distinguish cognitive tasks from physical load. The results are shown in Table 7 Cognitive tasks increased energy consumption of all subjects. Cognitive task during standing (T6) in the Lokomat increased all parameters significant from baseline standing (T1). Also cognitive task during walking (T7) increased all parameters compared to walking without cognitive task (T2, T3) but not significant. We conclude that ergospirometry can detect arousal in tasks without movements but it is not sensitive enough to assess arousal during tasks with physical load like walking.

Table 7: Results for ergospirometry measurements

	T1	**T2**	**T3**	**T4**	**T5**	**T6**	**T7**
VE (l/m)	10.1	18.3	21.0	44.9		17.5	31.1
Stdev	2.1	5.7	4.9	0.9		3.3	6.7
VT (l)	0.9	1.0	1.1	1.5		0.8	1.2
Stdev	0.4	0.2	0.3	0.2		0.1	0.3
RF (breath/min)	12.9	19.6	21.0	29.3		21.4	25.8
Stdev	6.6	6.5	7.4	3.8		3.2	3.5
R (dim less)	0.8	0.9	0.9	1.0		1.1	1.1
Stdev	0.1	0.1	0.2	0.1		0.1	0.3
VO_2 (l/m)	350.4	690.9	776.8	1814.1		506.4	923.3
Stdev	43.3	179.4	182.2	123.0		72.7	67.5
VCO_2 (l/m)	294.0	610.6	715.7	1786.2		546.6	1070.3
Stdev	29.7	126.2	156.2	287.9		65.9	333.0

4 Conclusion

The deliverable D3.1 covers two tasks in WP3 "Multi-sensorial data processing and decision making", namely task T3.1 "Principles and algorithms of real-time sensing of motor action and psychophysiological state" and task T3.2 "Real-time sensing of psychophysiological state". Please note that task T3.1 and T3.2 ran in parallel with WP1 "System specification and hardware setup", therefore, not all experiments were performed with the actual MIMICS set-up, since this was still under development.

The results of the task T3.1 are methods for real-time measurement of user's motor actions in a systematic modular way. Sensors acquire static and dynamic information such as forces/torques, positions and position derivatives, electromyographic (EMG) activity, as well as audio streams in order to record speech. Multi-sensorial integration algorithms were developed here in order to recognize the subject's voluntary motor activity and intention (intended movement direction) in real-time. The algorithms were validated on the actual MIMICS robotic systems.

The scope of the task T3.2 was measurement of the subject's psychophysiological state that would allow the system to determine how the subject is responding to the virtual environment and the therapy regime. The algorithms for real-time data acquisition and analysis were developed and evaluated in a group of volunteers. In the tasks related to upper extremities 20 participants were involved. In the lower extremities tasks 18 healthy volunteers were included. Since the actual MIMICS set-up was not complete to the point that would allow experiments at the time when the experiments were actually performed, a parallel experimental system was set-up that included the functionality of MIMICS device. Based on the results of the study it was possible to identify the most relevant physiological parameters to be used in the assessment of the user's psychophysiological state.

The results from tasks T3.1 and T3.2 will provide the basis for tasks T3.3 and T3.4. Task T3.3 will integrate all available measurements into one stream of data, while task T3.4 will build an expert decision making system based on the available measurements.

References

1. Andreassi, J. L., *Psychophysiology: Human behaviour and physiological response, 4th ed.* Lawrence Erlbaum Associates, Hillsdale, 2000.
2. Banz, R. et al., *Assessment of walking performance in robot-assisted gait training: A novel approach based on empirical data*. Proceedings of the 30th Annual International IEEE EMBS Conference, 2008 (in press).
3. Beauchaine, T., *Vagal tone, development and Gray's motivational theory: Toward an integrated model of autonomic nervous system functioning in psychopathology*. Development and psychopathology, Vol. 13, pp 183-214, 2001.
4. Boucsein, W., *The use of psychophysiology for evaluating stress-strain processes in human-computer interaction*. Engineering psychophysiology: Issues and applications, pp 289-309. Lawrence Erlbaum Associates, Mahwah, 2000.
5. Boucsein, W. and Backs, R., *Methods and Models for the Psychophysiology of Emotion, Arousal and Personality.* Handbook of Digital Human Modelling. Taylor & Francis / CRC Press, 2008 (in press).
6. Cacioppo et al., *The psychophysiology of emotion*. The Handbook of Emotion, 2nd ed., pp 173-191. Guilford Press, New York, 2000.
7. Fowles, D. C. et al., *Committee report: Publication recommendations for electrodermal measurements*. Psychophysiology, Vol. 18, No. 3, pp 232-239, 1981.
8. Fridlund, A. and Cacioppo, J., *Guidelines for Human Electromyographic Research*. Psychophysiology, Vol. 23, No. 5, pp 567-589, 1986.
9. Gomez, P. and Danuser, B., *Affective and physiological responses to environmental noises and music*. International Journal of Psychophysiology, Vol. 53, pp 91-103, 2004.
10. Hugdahl, K., *Psychophysiology. The Mind-body perspective.* Harvard University Press, Cambridge, 1995.
11. Jasper, H.H., *The ten-twenty electrode system of the International Federation*. Electroencephalography and Clinical Neurophysiology, Vol. 10, pp 370-375, 1958.
12. Kotchoubey B., Event-related potentials, cognition, and behavior: a biological approach. Neurosci Biobehav Rev 2006; 30: 42-65.
13. Köhler, B.U., Hennig, C. and Orglmeister, R. *The principles of software QRS detection*. IEEE Engineering in Medicine and Biology, Vol. 21, No. 1, pp 42-57, 2002.
14. Kreibig, S. et al., *Cardiovascular, electrodermal, and respiratory response patterns to fear- and sadness-inducing films*. Psychophysiology, Vol. 44, pp 787-806, 2007.
15. Laarni, J. et al., *Using eye tracking and psychophysiological methods to study spatial presence*. Proceedings of the 6th International Workshop on Presence, Aalborg, 2003.
16. Larsen et al., *Effects of positive and negative effect on electromyographic activity over zygomaticus major and corrugators supercilii*. Psychophysiology, Vol. 40, pp 776-785, 2003.

17. Malmivuo, J. and Plonsey, R., *Bioelectromagnetism: Principles and Applications of Bioelectric and Biomagnetic Fields.* Oxford University Press, New York, 1995.
18. Mandryk, R., *Using psychophysiological techniques to measure user experience with entertainment technologies*. Behaviour & Information Technology, Vol. 25, No. 2, pp 141-158, 2006.
19. Min, B.C. et al., *Autonomic responses of young passengers contingent to the speed and driving mode of a vehicle*. International Journal of Industrial Ergonomics, Vol. 29, pp 187-198, 2002.
20. Mulder et al., *A psychophysiological approach to working conditions*. Engineering psychophysiology: Issues and applications, pp 139-159. Lawrence Erlbaum Associates, Mahwah, 2000.
21. Ohsuga, M. et al., *Assessment of phasic work stress using autonomic indices*. International Journal of Psychophysiology, Vol. 40, pp 211-220, 2001.
22. Rimm-Kaufmann, S.E. and Kagan, J., *The psychological significance of changes in skin temperature*. Motivation and Emotion, Vol. 20, pp 63-78, 1996.
23. Romet, T. T. and Frim, J., *Physiological responses to fire fighting activities*. European Journal of Applied Physiology, Vol. 56, pp 633-638, 1987.
24. Rousselle JG, Blascovich J, Kelsey RM. Cardiorespiratory response under combined psychological and exercise stress. Int J Psychophysiol 1995; 20: 49-58
25. Rose, R. M. and Fogg, L. F., *Definition of a responder: Analysis of behavioral, cardiovascular and endocrine responses to varied workload in air traffic controllers*. Psychosomatic Medicine, Vol. 55, pp 325-338, 1993.
26. Schumacher, A., *Master thesis in human biology: Cortical control of human walking – An electroencephalography (EEG) study with healthy subjects*. University of Zurich, Zurich, 2008.
27. Schwartz, G. E. et al., *Cardiovascular differentiation of happiness, sadness, anger and fear following imagery and exercise*. Psychosomatic Medicine, Vol. 43, pp 343-364, 1981.
28. Simons, R. F. et al., *Emotion processing in three systems: The medium and the message*. Psychophysiology, Vol. 36, pp 619-627, 1999.
29. Task Force of the European Society of Cardiology and the North American Society of Pacing and Electrophysiology, *Heart rate variability: Standards of measurement, physiological interpretation, and clinical use.* European Heart Journal, Vol. 17, pp 354-381, 1996.
30. Thayer, J.F. and Lane, R.D. *A model of neurovisceral integration in emotion regulation and dysregulation*. Journal of Affective Disorders, Vol. 61, pp 201-216, 2000.
31. Turpin, D., *Ambulatory psychophysiological monitoring: Techniques and applications.* Experimental and Clinical Psychophysiology, pp 700-728. Croom Helm, London, 1985.
32. Van Reekum et al., *Psychophysiological responses to appraisal dimensions in a computer game*. Cognition & Emotion, Vol. 18, pp 663-688, 2004.
33. Veltman, J.A. and Gaillard, A. W. K., *Physiological workload reactions to increasing levels of task difficulty*. Ergonomics, Vol. 41, pp 656-659, 1998.